1-1-2015

A survey and study of planar antennas for pico-satellites

Faisel Em M Tubbal
University of Wollongong, femt848@uowmail.edu.au

Raad Raad
University of Wollongong, raad@uow.edu.au

Kwan-Wu Chin
University of Wollongong, kwanwu@uow.edu.au

A survey and study of planar antennas for pico-satellites

Abstract

Works on pico-satellites have gained momentum recently, especially those that consider pico-satellites as part of a much larger constellation or swarm. This feature allows pico-satellites to provide high temporal resolution of observational data and redundancy. In particular, it reduces the need for satellite-to-ground communications and, hence, helps save energy and allows the execution of distributed processing algorithms on the satellites themselves. Consequently, satellite-to-satellite or cross-link communication is critical. To realize these advantages, the cross-link antenna employed on pico-satellites must meet many criteria, namely, small size, lightweight, low-power consumption, high gain, wide bandwidth, circular polarization, and beam steerability. To date, no works have examined the suitability of existing planar antenna designs for the use on pico-satellites. To this end, this paper contributes to the literature by focusing on microstrip patch and slot antennas that have the ability to achieve high gain, beam steering, and wide bandwidth. This paper reviews 66 planar antenna designs, which includes 38-patch and 28-slot antennas. In addition, we provide an extensive qualitative comparison of these antennas in terms of their mass, size, gain, beam steerability, type of polarization, operating frequency band, and return loss. In addition, we have evaluated three antenna designs that best address the pico-satellite challenges on a common platform. We find that the asymmetric E-shaped patch antenna design is the most suitable for the use on 2U CubeSats. This is because of its small size ($34times 13$ mm $^{2})$ and high gain (7.3 dB). In addition, the E-shaped patch antenna yields a wide −10-dB bandwidth of 2300 MHz and a small return loss of −15.2 dB.

Keywords

study, planar, antennas, pico, survey, satellites

Disciplines

Engineering | Science and Technology Studies

Publication Details

F. Em . Tubbal, R. Raad & K. Chin, "A survey and study of planar antennas for pico-satellites," Access IEEE, vol. 3, pp. 2590-2612, 2015.

IEEE Access
The journal for rapid open access publishing

Received October 27, 2015, accepted November 17, 2015. Date of current version December 17, 2015.

Digital Object Identifier 10.1109/ACCESS.2015.2506577

A Survey and Study of Planar Antennas for Pico-Satellites

FAISEL EM TUBBAL, (Member, IEEE), RAAD RAAD, (Member, IEEE), AND KWAN-WU CHIN, (Member, IEEE)
School of Electrical, Computer and Telecommunications Engineering, University of Wollongong, Wollongong, NSW 2522, Australia
Corresponding author: F. EM. Tubbal (femt848@uowmail.edu.au)

ABSTRACT Works on pico-satellites have gained momentum recently, especially those that consider pico-satellites as part of a much larger constellation or swarm. This feature allows pico-satellites to provide high temporal resolution of observational data and redundancy. In particular, it reduces the need for satellite-to-ground communications and, hence, helps save energy and allows the execution of distributed processing algorithms on the satellites themselves. Consequently, satellite-to-satellite or cross-link communication is critical. To realize these advantages, the cross-link antenna employed on pico-satellites must meet many criteria, namely, small size, lightweight, low-power consumption, high gain, wide bandwidth, circular polarization, and beam steerability. To date, no works have examined the suitability of existing planar antenna designs for the use on pico-satellites. To this end, this paper contributes to the literature by focusing on microstrip patch and slot antennas that have the ability to achieve high gain, beam steering, and wide bandwidth. This paper reviews 66 planar antenna designs, which includes 38-patch and 28-slot antennas. In addition, we provide an extensive qualitative comparison of these antennas in terms of their mass, size, gain, beam steerability, type of polarization, operating frequency band, and return loss. In addition, we have evaluated three antenna designs that best address the pico-satellite challenges on a common platform. We find that the asymmetric E-shaped patch antenna design is the most suitable for the use on 2U CubeSats. This is because of its small size (34×13 mm^2) and high gain (7.3 dB). In addition, the E-shaped patch antenna yields a wide -10-dB bandwidth of 2300 MHz and a small return loss of -15.2 dB.

INDEX TERMS Circular polarization, reconfigurable antennas, antenna arrays, beam steering, CubeSat, pico-satellites, planar antennas, microstrip patch antennas, sequential phase-rotation, photonic band-gap (PBG).

I. INTRODUCTION

Conventional polar orbiting satellites operate at altitudes of 800 to 900 km and are sun synchronous, crossing the equator at the same local time every day with an orbital velocity of about 7.8 km/s. They are mainly used for (i) communications; e.g., mobile telephony, or (ii) remote sensing; e.g., land imaging and weather forecasting. Another application is military, where they are used for spying, watching the borders of countries, and to enable secure communications [1]. As shown in Table 1, these conventional satellites are relatively large, heavy with most weighing in at above one tonne, and have high power consumption in the range of 1 kW. Moreover, they are able to carry high gain (usually parabolic) antennas for ground communications, and their typical life cycle exceeds 10 years. Lastly, they are very expensive, costing upwards of one billion dollars [2].

In contrast, pico-satellites (picosats) are extremely small, and lightweight. They have a wet mass between 0.1 and 1.33 kg. In this respect, CubeSats [1] are the largest and most popular. Fig. 1 depicts a 10-cm CubeSat with a mass of no more than 1 kg. All CubeSats have a fixed size of 10cm $\times$ 10cm with three different lengths: 10cm, 20cm, and 30cm. These lengths correspond to the requirement of the Poly-Pico-satellite Orbital. Deployer (P-POD) [3]. Consequently, they can be deployed from standard rockets or more recently from the International Space Station (ISS) [4]. Indeed, they can be placed in a single launcher tube. A launch vehicle carrying such a tube can then simply release the satellites upon reaching their target orbit. Compared with conventional and medium sized satellites, as set out in Table 1, they cost less, and are easy to construct but have fewer capabilities. Interestingly, CubeSats can be networked to form satellite constellations or swarms. They can jointly maintain a fixed or relative position with each other in a distributed manner [5]. This is particularly advantageous for sensing applications because a swarm of CubeSats can

IEEE Access
The journal for rapid open access publishing

TABLE 1. Classification of small satellites.

	Type	Mass (kg)	Cost (US $)	Time to Build	Antenna Gain	Power Consumption
	Conventional	>1000	0.1-2 B	>5 years	Very high	~ 1000 W
	Medium	500-1000	50-100 M	4 years	Very high	~ 800 W
Small Satellites	Mini	100-500	10-50 M	3 years	High	53.2W
	Micro	10-100	2-10 M	~ 1 year	Medium	35 W
	Nano	1-10	0.2-2 M	~ 1 year	Medium	7 W
	Pico	1-1.3	20-200 K	<1 year	Low	2 W
	Femto	<0.1	0.1-20 K	<1 year	Low	6 mW

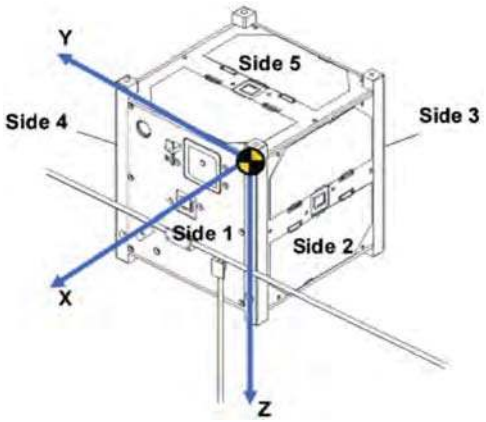

FIGURE 1. A cube satellite (10cm × 10cm × 10cm) [15].

take multiple and distributed measurements. An example of a CubeSat swarm is RapidEye, which is a commercial venture with a constellation of five mini-satellites deployed in 2008 and operate in the low earth orbit (LEO) (630 km) [2]. In another example, the authors of [6] and [7] reported the launch of six aerospace pico-satellites by Stanford University using an orbiting automated pico-satellite launcher. Four of these pico-satellites have a dimension of 4 × 3 × 1 cubic inches, and the other two measure 8 × 3 × 1 cubic inches. Notably, the entire launch costs only $30,000 [8].

To date, pico-satellites have found applications in fields such as education and scientific experiments. Specifically, pico-satellite programs provide education and training to students, scientists and engineers in space related skills; e.g., design production, test, launch and orbital operations of satellites. Many universities and engineering schools in Europe, Japan, and the United States of America have already developed, launched and operated their own pico-satellites. For example, Picpot [9] is an educational pico-satellite built at the Politecnico di Torino University. In particular, pico-satellites are good examples of a complex system with specific constraints and requirements. Consequently, building one allows students to learn the techniques and procedures related to pico-satellites development. Other uses of pico-satellites include remote sensing applications. For example, ocean altimetry measurements, remote sensing of sea ice, land and ocean temperature measurements, environmental disaster monitoring, atmospheric temperature and humidity measurements [10]. One example is the Disaster Monitoring Constellation (DMC) project [8], [11]. It consists of six micro satellites that are used to monitor and mitigate man-made and natural disasters; e.g., the Indian Ocean tsunami in 2004. Apart from that, the international community is working to form and launch swarms of pico-satellites. One example is the QB50 project, which is collaboration between 15 different partners from all over the world [12]–[14]. Its aim is to provide affordable access to space and in-situ measurements of Earth's lower thermosphere/ionosphere region.

There are many criteria and challenges when designing pico-satellites. The primary ones are listed in Tables 2 and 3. Their limited size means only a small area is available for solar cells, which in turn limits the generated power that feeds all components. The other challenge is the small power budget of usually no more than 2W, which limits or entirely eliminates backup units. Consequently, pico-satellites have low reliability, and hence, they have a short lifetime ranging from a few weeks to a few months [16]. As a result, pico-satellites need to operate autonomously and must be able to handle any anomalies that occur. They also need to be equipped with lightweight and small antennas that provide gain and wide bandwidth. This is important for communications between satellites and ground stations.

To date, past works on antenna designs for small satellites have considered four different antenna types. They include:

i) *Omni-directional*. They are required by the Telemetry, Tracking and Command (TTC) subsystem, which facilitates space to ground communications. They include monopole, patch-excited cup and helix antennas. These antennas, however, usually require high power consumption as they radiate in all directions. They also occupy a large area. As a result, pico-satellites typically use lightweight and small sized microstrip patch and slot antennas for TTC [19], [20].

ii) *High gain*. These antennas are mainly used for high speed down-links to ground stations. High data rates require an antenna with a gain of about 12 dB [19]. However, the very limited space and power on pico-satellites make it difficult to accommodate such a high gain antenna as it requires high power for its active circuits and occupies a large area. The most common type of high gain antennas used by conventional satellites is a horn antenna with a pointing mechanism

TABLE 2. Pico-satellites system challenges and their importance.

Challenges	Implications	Operating Ranges
Small size	• Limited surface area, primarily used for solar cells, meaning the energy harvesting rate is small, which in turn affects operational lifetime. • Constrains available resources such as batteries, and hence, affects mission durability. • Bounds on antenna size.	$\leq 10\times10\times10\ cm^3$
Small mass	• Limits the size and capacity of battery, which in turn bounds the power budget of communication components. • Precludes the use of standard Attitude Determination and Control Systems (ADCS) for pico-satellites with mass less than 1.3 kg [17]. • Obviate the use of high gain, and usually heavy, directional horn antennas. Moreover, additional weight will be incurred if satellites are equipped with complicated reflectors and arrays to achieve high gains.	≤ 1.3 kg
Limited power	• Mass and surface area restrictions affect the amount of generated power from solar cells, which in turn limits redundancy. • Limits the use of high performance, but power hungry, elements such as steering arrays and ADCS. • Low hardware redundancy, and hence, increases the probability of system failure.	≤ 2 W
Limited bandwidth and communication opportunities	• Affect applications that require high data rates. For example, mapping, and downloading high resolution images to a ground station [18]. • Reduced transmission capacity due to the loss of contact with ground stations.	1.2 – 9.6 kbit/s

TABLE 3. Antenna design challenges for pico-satellites.

Design Properties	Performance	Relevant Works
Small size and low mass	• Low power consumption, easy to construct, cheap, occupy a small area, and provides sufficient real estate to mount solar cells. • Do not dominate the satellite profile or weight budget.	[23-39]
Circular polarization	• Eliminates polarization mismatch losses. • Only 3 dB loss regardless of antenna orientation.	[23-29], [35-37] and [40-51]
Impedance matching	• Maximize power transfer or equivalently, minimize power loss. • Minimize signal reflection.	[23-38, 40-54]
High gain and wide bandwidth	• Long distance communication, increased contact period with ground stations. • Enable inter-satellite communications.	[23, 24], [27-29], [35-37], [39-50] and [53]
Frequency re-configurability	• The ability to radiate more patterns at different frequencies and polarizations to enhance system performance.	[48] and [53].
Beam steerabilty	• Saves power by directing an antenna's beam to a desired direction.	[37], [40], [44, 45], [47] and [49]

and S-band quadrifilar-helix antennas; see [19]. In addition, the authors of [21], proposed a high gain deployable hemispherical helical antenna for Cube-Sat to ground communications. However, as set out in Table 5, amongst all patch and slot antennas, their highest gain is 12.45 dB. Consequently, pico-satellites use small microstrip patch and slot antennas.

iii) *Medium-gain and low backward radiation.* These antennas are mainly used by receivers in the Global Positioning System (GPS) to ascertain the position, velocity, and timing of pico-satellites in LEO. Many types have been developed; namely, patch-excited cup and shorted–annular patch antennas. They have a gain of about 12 dB, operate at 1.575 and 1.227 GHz and have a small size. Also, they produce low back radiation to minimize interference with satellite components. Recently, in [19], the authors presented a Geohelix ceramic loaded quadrifilar-helix antenna. However, despite its small size, the resulting antenna has a low gain.

iv) *Directive self-steering*. The main function of these antennas is to provide circular polarization (CP) in

order to establish communication links between satellites. Furthermore, beam steering techniques can be employed to increase directivity and achieve higher gains [19]. In this respect, pico-satellites use self-steering. In contrast, conventional satellites employ dynamic beam steering [22].

In this paper, we present a unique collection of techniques and approaches that apply to microstrip patch and slot antennas in order to achieve miniaturization, high gain and wide bandwidth. We note that existing planar antenna designs have not been compared and evaluated in terms of their suitability for pico-satellite communications. Therefore, we first present and classify patch and slot antennas based on their approaches and techniques. We then compare their performance in terms of suitability for pico-satellite communications. Our contributions are as follows: (i) we review 66 planar antenna designs, which include 38 patch and 28 slot antennas, (ii) we provide an extensive qualitative comparison in terms of gain, volume, mass, beam steerability, polarization, operating frequency and return loss, (iii) we identify micro-strip patch and slot antennas that are suitable for pico-satellites, i.e., those that meet some or all of the criteria listed in Table 3, (iv) we compare and evaluate the most suitable antenna designs by implementing and testing these designs on a common platform. Critically, we study how their performance is affected by a 2U CubeSat body. We compare and evaluate these designs with and without a 2U CubeSat and recorded their performance in terms of volume, gain at 2.45 GHz, bandwidth, return loss, robustness, beam steerability and cost.

The remainder of this paper has the following structure. Section 2 introduces a comprehensive taxonomy of the main challenges and solutions in designing patch and slot antennas. We classify them according to their alibility to achieve high gain and steerability, wide bandwidth, and small size. Section 3 provides a qualitative evaluation and a comparison between all designs. Section 4 presents a quantitative evaluation between the most suitable designs. The paper concludes with Section 5.

II. MICRIOSTRIP PATCH AND SLOT ANTENNAS

There is growing interest in planar antennas that are easily integrable with other RF and microwave circuits. However, using planar antennas for pico-satellite communications has many challenges in terms of gain, bandwidth and antenna size; specifically those outlined in Table 3. In the sequel, we present their designs, problems solved, advantages and limitations.

A. MICROSTRIP PATCH ANTENNAS

Fig. 2 shows a typical microstrip patch antenna that consists of a metal ('Patch') on the top of a grounded dielectric substrate. This patch can be made of different shapes; rectangular being the most common shape. Moreover, the patch antenna is fed by a microstrip transmission line. The patch and feed line are usually made from copper. Patch antennas have been used

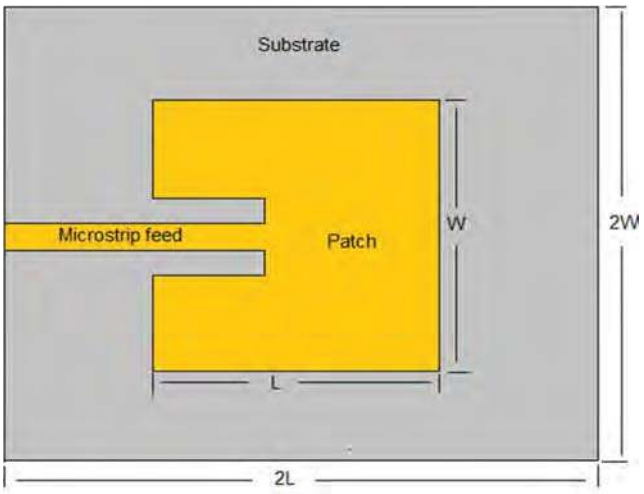

FIGURE 2. A microstrip patch antenna.

for different applications. They include medical [55], [56], CubeSat; i.e., earth observation [30], and military applications, i.e., elements array in radar scanning [55]. To date, we have identified eighteen designs aimed at microstrip patch antennas with the goal of achieving beam steerability, increasing gain, reducing their size, and enhancing supported bandwidth. As Table 4 shows, all these designs achieve gains ranging from 1.53 to 18 dB, with an antenna size ranging from $3.14\times0.8^2\times0.078\ cm^3$ to $12\times16.8\times2.5cm^3$. Moreover, they work in the L, S, C and X frequency bands (1 – 14.15 GHz). In terms of gain and size, most of these designs are suitable for pico-satellites communications.

Amongst all microstrip patch antenna designs we report later, i.e., those in [23], [24], [26], [28], [30], [31], [34], [39]–[42], [44], [45], [47], [49]–[51], and [57]–[62], the one in [49] has the highest gain at 18 dB and operates in the 6.175 GHz. However, its size, i.e., $16\times16\times0.35cm^3$, rules it out for use by pico-satellites. On the other hand, the design in [24] has the smallest dimension at $2.7\times2.7\times0.0892\ cm^3$ and a high gain of about 6 dB. In terms of operating frequency, all the designs in [23], [24]–[26], [28], [30], [31], [34], [39]–[42], [44], [45], [47], [49]–[51], and [57]–[62] are suitable for satellite links and wireless communication applications as they operate in the super high frequency (SHF) band (2-30 GHz). However, the most suitable frequency band for pico-satellites is the S-band (2-4 GHz). Moreover, one limitation of the antenna designs in [23], [25], [26], [28], [30], [31], [34], [39], [41], and [51] is the lack of steerability. This is very important for cross links, and secure communications.

We will further discuss these proposals in more details in terms of their gain and steerability in Section 2.1.1. Then in *Section 2.1.2,* we present antennas that have high bandwidth while *Section 2.1.3* presents those that are size sensitive.

1) STEERABILITY AND GAIN IMPROVEMENT

Recently, beam-steerable and high gain antennas have received considerable attention due to their enhanced

TABLE 4. Different microstrip patch antenna designs and their performance.

Reference	Gain (dB)	Volume (cm^3)	Band (GHz)
Osorio et al. [47]	6.9	9×9×0.5	C-Band (5.8)
Ma et al. [44]	7.5	15×15×0.96	S- Band (2.37)
Hu et al. [49]	18	16×16×0.35	C-Band (6.175)
Nascetti et al. [30]	5.9	3.97×1.2×0.21	S-Band (2.45)
Mizuno et al. [45]	6.25	10×10×0.16	C-Band (10.5)
Budianu et al. [40]	4.8	10×10×0.16	S-Band (2.45)
Qian et al. [50]	5.02	12×16.8×2.5	Ku-band (14.15)
Montaño et al. [51]	n/a	8.01×8.01×2.25	S-Band (2.40)
Iwasaki [42]	6	7×7×0.16	L-Band (1.525)
Ferrero et al. [24]	6.2	2.7×2.7×0.0892	S-Band (3.5)
Massa et al. [41]	5.9	8.8×8.8×2.5	C-Band (4.32)
Chiu et al. [23]	2.58 or 2.4	≈ 5.4×5.4×0.7 and ≈ 4×4×0.7	C-band (3.5-6.5)
Malekpoor et al. [28]	4.9 or 3.9	2.8 ×1×0.7 and 1.8×1.5×0.7	UWB (3.57-11.98)
Holub et al. [26]	n/a	2.21×2.21×1.5	L-band (1.575) UHF-band (0.869)
Ouedraogo et al. [34]	5.96 (1.2cm), 4.86 (0.8cm), and 4.23 (0.6cm)	$3.14 \times 0.8^2 \times 0.078$	S- band (2.45)
Addaci et al. [31]	n/a	$3.14 \times 2.7^2 \times 1.37$	S- Band (2.4-2.5)
Rahmadani et al. [25]	1.53	3.8 ×3.8	S- Band (2.45)
Malekpoor et al. [39]	8	3.4 ×1.3×0.7	C-Band (6.73)

radiation performance and suitability for long distance communications. The main techniques used to achieve beam steering include sequential phase-rotation, retrodirective array [45], beam forming algorithm [40], and for increasing gain, photonic band-gap (PBG) structures [50], and single proximity coupled feed [42]. We note that conventional pointing mechanisms, such as [47], for steering antenna beams are not suitable for use by pico-satellites because of their size and mass constraints.

a: SEQUENTIAL PHASE-ROTATION

Sequential phase-rotation is a popular approach. The main idea is to feed each sub-array element sequentially by making adjacent patches orthogonally oriented (90°) to achieve CP at the following phases: 0°, 90°, 180°, and 270°. In [47], Osorio et al. propose a square antenna array with nine identical elements (3 × 3). Each element is formed by a 2 × 2 sub-array of rectangular patches. Adjacent patches are orthogonally oriented to provide CP. Beam steerability is achieved by feeding the sub-arrays at 0°, 90°, 180°, and 270° using a phase shifter. They reported beam steerability and a high gain of 6.9 dB. The use of rectangular patches leads to a reduction in mutual coupling between adjacent patches. This improves performance due to the isolation between antenna arrays. This also leads to a reduction in interference between array elements. Its main limitation, however, is the low coupling between the feed line and the radiating patch. This significantly affects impedance matching and radiating efficiency. To solve this problem, Osorio et al. propose moving the feed line slot back to the centre of the patch where the coupling through the electrical dipole is maximized. Another limitation is its inability to switch between two different polarizations, which is an important feature as it helps enhance the reception of weak signals.

Microstrip arrays can provide various radiation characteristics with their feed networks, which are often designed using power dividers (or a combiner) to deliver a RF signal with specific amplitude and phase to each radiating element. In [44], Ma et al. propose a technique to achieve polarization diversity and an electrically steerable radiation pattern. The main approach is a three quasi-lumped couplers and a 90° phase delay line. The operation of these couplers can be switched between the T-junction divider mode and 3-dB hybrid mode by controlling the capacitance value of the lumped capacitors. By connecting this feed network to four rectangular radiating elements of the microstrip array, the T-junction divider provides linear polarization while a 3-dB hybrid [63] provides CP. This is important as it achieves the best signal strength and mitigates multipath fading. Moreover, the beam steering capability of circular polarisation allows a link to be established when re-orienting two satellites. It is interesting to note that steerability and high gains of 7.1dB and 7.5 dB are obtained for CP and LP respectively. One major drawback is the antenna size, i.e., $15 \times 15 \times 0.96 cm^3$, which exceeds the size of pico-satellites.

Power dividers, which distribute power to different radiating elements, facilitate beam steering control. In [49], Hu et al. use a two-way Wilkinson power divider [64] to feed a network array that has sequential rotated elements. This power divider provides high isolation and 90° phase shift between adjacent radiating elements and sub-arrays. This is important as it achieves broadband CP at high gains. They reported beam steerability, wide bandwidth and a superior gain of 18 dB. This design achieves wider bandwidth and

much higher gain than the designs presented in [44] and [47]. Compared to [44], which uses a three-port power divider, the two-way divider in [49] occupies a smaller area because it reduces the total size of the feeding network layout. Its main limitation is the large antenna size (16cm $\times$ 16cm $\times$ 0.35cm). This has a non-negligible impact on the actual surface area used for solar cells, and hence energy harvesting rate, which in turn affects operational lifetime. Another limitation is the use of a 90° phase shifter, which has a significant impact on cost, dimension and is complex to control.

One of the most popular power divider designs is the Wilkinson power divider [65]. It splits the input power signal into n signals of equal amplitude and phase, and is commonly applied in antenna array systems that require corporate or parallel feed systems. In [30], Nascetti et al. used a Wilkinson structure to design a power divider that feeds a network array of four identical patches placed on 1U CubeSat face. This power divider design provides a high isolation between the output ports at good impedance matching. The main idea is to feed every two adjacent patches that are orthogonally oriented (90°) using a power divider to achieve CP at high gain. This is important as it increases the reception and signal strength; it thus helps establish communication links with a ground station and other CubeSats. The design achieves a maximum gain of 5.9 dB and a return loss of -15.05 dB at an operating frequency of 2.45 GHz for a single patch. Moreover, the authors used all four patches to achieve a high gain of 7.3 dB and a small return loss of -25 dB at 2.45 GHz. Compared to the designs in [44], [47], and [49], the one reported in [30] has a much smaller antenna size, i.e., 3.97 $\times$ 1.2 $\times$ 0.21cm^3, and less complex. However, its main limitation is the implementation of the antenna design on only one face of the CubeSat. This means directivity is maximized in one direction, meaning no cross-links communications when CubeSats are oriented toward a ground station.

b: RETRODIRECTIVE (SELF-STEERING)

Approaches that use retrodirective arrays [66]–[68] are becoming popular due to their simplicity as compared to those that use phased-array and smart antennas. Specifically, retrodirective antennas are able to reflect an incident signal towards the source direction without any prior location information. In [45], Mizuno et al. use a retrodirective (self-steering) array. This technique is an alternative to dynamic beam steering and also helps increase gain. We note that conventional phased-array antennas use phase shifters to achieve beam steerability. In contrast, retrodirective arrays steer their beams by sensing the incoming signal without the need for phase shifters. Consequently, they are cheaper, less complex, lighter, and smaller in size. Compared to smart antennas that rely on digital signal processing for beam control, e.g., [44], [47], [49], retrodirective array systems are much simpler and potentially faster because it does not require computation. However, its main limitation is the use of a high local frequency that is set to twice the incoming radio frequency. Hence, this incurs high power, which is a key limitation of pico-satellites due to their scarce energy resource.

c: BEAM FORMING ALGORITHM APPROACH

Different antenna array systems use beam forming algorithms to control radiation patterns. Budianu *et al.* [40] propose to install a micro-strip patch antenna on each face of cube satellites. Each antenna provides CP. A beam forming algorithm is then used to identify a spatial signal signature. This is important as it maximizes directivity for any link direction. Also, the use of six antennas ensures a communication link remains available at all times regardless of CubeSats orientation. Compared to the designs in [44], [47], and [49] that use complex digital signal processing and a phase shifter to steer beams, beam forming algorithms are more simple as they are based on simply adding the electrical fields of adjacent antennas, and hence, have a high gain. However, this approach occupies precious space that otherwise could be used for solar cells.

d: PHOTONIC BAND-GAP (PBG) STRUCTURES

Surface-wave losses in patch antennas lead to a decrease in radiation efficiency and gain. Therefore, surface-wave suppression techniques are needed to enhance radiation pattern efficiency. Most of these techniques are related to periodic structures [69]–[73]. The most popular one are Photonic band-gap (PBG) structures [74]. In [50], Qian et al. propose to surround a patch antenna with a square-lattice of small metal pads. This leads to a substantial suppression of surface waves excited in the dielectric substrate. They reported a radiation efficiency of 85% and a gain of 5.02 dB. In general, this technique achieves wider bandwidth, higher gain, lower backside radiation, beam shape control and surface wave suppression. Unfortunately, the resulting antenna is not steerable.

e: SINGLE PROXIMITY COUPLED FEED

A proximity coupled feed technique is used to transfer power between the microstrip line and the radiating patch based on electromagnetic field coupling [75]. In [42], Iwasaki presents a design for a circularly polarized patch antenna with a single proximity couple feed line. This antenna has a cross slot with unequal lengths on its patch. A single proximity coupled feed is an electromagnetically coupled method. This electromagnetic field coupling is carried out to transfer power between the microstrip line and the radiating patch. This leads to higher isolation between the DC supply and RF signal. It achieves a CP without the need for an external circular polarizer. This is important as it is less complex and incurs less weight and size. Iwasaki reported a high gain of 6 dB at CP which is important for cross-link communications in pico-satellites. Another advantage is the ability to control gain, resonant frequency and antenna size.

2) ANTENNA BANDWIDTH ENHANCEMENT

The main techniques used to enhance bandwidth include agile polarization [24], cavity [41], U-slot and

L-slit geometries [23], folded-patch approach [28], and transparent mesh line geometry [51]. All these techniques achieve significant enhancement in bandwidth ranging from 3.8% in the 3.8 GHz frequency band to 98.22% in bands ranging from 4 to 11 GHz. Moreover, these approaches have no significant effect on antenna size.

a: AGILE POLARIZATION

Antennas of this type are able to dynamically change their polarization state, i.e., they can have either linear (vertical or horizontal) or CP (left or right hand) [59]. In [24], Ferrero et al. designed a novel quad-polarization agile patch antenna to achieve simple polarization reconfigurability and to enhance bandwidth. The main approach is to feed a radiating patch with two orthogonal slots that are excited by a tuneable quasi-lumped coupler (QLC). These couples can be switched between two different operating modes: 3-dB hybrid coupler and directional coupler via a DC bias voltage to achieve agile polarization capabilities. This is important as it addresses multipath fading. The resulting antenna has a wide 3 dB axial ratio CP bandwidth of 3.8% with respect to the centre frequency of 3.5 GHz.

b: CAVITY MODEL

This technique is used to analyze microstrip patch geometry and to provide a better way to model radiation patterns [61]. In [41], Massa et al. develop a cavity model for a printed annular patch antenna to achieve higher bandwidth and simplified match feeding system. The key idea is to connect (shorting) the inner edge of the annular patch antenna by a cylindrical conducting wall. This in turn reduces the antenna's stored energy. As bandwidth depends on the ratio between the radiated power (P_r) and stored energy (W_t) of the antenna ($BW = P_r/W_t$), reducing the amount of stored energy leads to an increase in bandwidth. This is important for systems requiring wider coverage; e.g., in [40] the authors use six antennas on the surface of pico-satellites to achieve a wide bandwidth in order to establish crosslinks between satellites. The main advantage is their low impedance around their edge, which allows the use of a coplanar microstrip without the need for an external matching network. This is important as it simplifies the whole design and enhances matching capability. In addition, the annular antenna design in [41] works as a circular patch antenna to provide circular or double polarization. Moreover, annular design provides wider bandwidth and better coverage.

c: U-SLOT AND L-SLIT GEOMETRIES

U-slot and L-slit are two common geometries employed by antennas with dual-band operation as they help enhance bandwidth [62]. In [23], Chiu et al. propose two approaches based on U-slot and L-slot geometries to enhance the bandwidth of a conventional quarter-wave patch antenna. The key idea is to include a folded inner small patch within the larger patch. Also, shorting walls are used to reduce the overall size of the antenna to nearly a quarter wavelength of the centre operating frequency (3.5 to 6.5 GHz). This is important because it increases bandwidth and reduces antenna size. Chiu et al reported a significant enhancement in bandwidth with a voltage standing wave ratio (VSWR) of less than two. The bandwidth of a U-slot antenna is 53.54% (3.57 to 6.18 GHz) while for L-slit it is 45.12% (4.265 to 6.75 GHz). Compared to the microstrip patch antenna designs in [24] and [41], the one reported in [23] has a much wider bandwidth than the design in [41] and smaller than that of [24].

d: FOLDED-PATCH FEED

Folded-patch feed is used by ultra-wideband (UWB) patch antennas [57], [58], [60]. In [28], Malekpoor et al. use two different approaches to design shorted patch antennas with significant enhancement in impedance bandwidth. The first approach is to feed unequal resonance arms of the upper patch by a folded ramp-shaped patch. This helps enhance bandwidth without incurring any increase in patch size. In the second approach, they use a folded ramp-shaped feed and one pin in the centre of the upper patch to increase bandwidth. They also use shorting pins between the patches and the ground plane to miniaturize their size. They reported a significant enhancement in impedance bandwidth; specifically 94.17% at 4.13 to 11.48 GHz, and 98.22% at 3.57 to 10.46 GHz, for first and second techniques respectively. This is very important as they enable high data rates. Compared to the designs in [23], [24], and [41], the proposed antenna in [28] has a much wider bandwidth, i.e., 3.57 to 10.46 GHz and is smaller in size, i.e., $2.8 \times 1 \times 0.7$ cm^3 and $1.8 \times 1.5 \times 0.7$ cm^3.

e: TRANSPARENT MESH LINE GEOMETRY

A meshed structure is an alternative to those that are made of transparent materials. They have high transparency; i.e., 80% and good efficiency; i.e., 50% [76]. Montaño *et al.* [51] propose a transparent mesh printed patch antenna design to be placed on the face of 3U CubeSat for downlink or ground communications. The designed antenna consists of a 4.34 cm^2 square meshed lines on a 8.01 cm^2 squared ground plane. The main idea is to implement copper grid lines on a high transparent substrate; i.e., quartz material. The resulting meshed antenna is then placed underneath solar cells. This is very important as it maximizes the efficacy of the solar panels. Moreover, the gain, operating frequency, efficiency, and bandwidth are enhanced by varying the mesh lines width. Montaño et al. reported a bandwidth of 80 MHz and return loss of -22 dB at a resonance frequency of 2.4 GHz. Compared to the designs in [23], [24], [28], and [41], the proposed antenna design in [51] provides more space for solar cells; i.e., its affords a CubeSat more power.

3) PATCH ANTENNA MINIATURIZATION

The main techniques used to reduce antenna size include meandering [26], metamaterial [34], cylindrical skirts with shorting pins [31], artificial magnetic conductor [25] and shorting pins [39]. These techniques are capable of

reducing the antenna size by $3.14 \times 0.6^2 \times 0.078$ to $3.14 \times 2.7^2 \times 1.37 cm^3$.

a: MEANDERING

The main advantage of meandering is the reduction in microstrip patch antenna size whilst maintaining the same resonant frequency. In [26], Holub et al. present a novel design technique to miniaturize microstrip patch antennas. The main approach is to use a multilayer meanderly folded shorted patch structure. This means repeatedly folding the cavity of conventional patch antenna and hence, the electrical length of the whole N-times folded cavity and the resonant frequency remains constant. This decreases the original shorted (quarter-wavelength) patch by 1/N, where N is a number of vertically placed patch plates. Also, the resonant frequency of the antenna does not change. This is important as there is a constant demand for small antennas that operate at high frequencies; e.g., distributed pico-satellites systems [77]. Holub et al. tested two antenna prototypes; the first design has two cavity meanders and resonant frequency of 1.575 GHz. The second design has three cavity meanders and resonant frequency of 0.869 GHz. They reported two structures with physical lengths of 2.21cm and 1.63 cm. This is a significant achievement as these physical lengths are much smaller than those in conventional rectangular patch antennas (9.52cm).

b: METAMATERIAL

This is an important technique as it provides higher levels of miniaturization such as negative permeability metamaterial, μ-negative (MNG) metamaterial, a volumetric metamaterial and magneto-dielectric embedded-circuit meta-substrate [78]–[81]. Ouedraogo *et al.* [34] introduce a new design methodology that produces highly miniaturized patch antennas with a low profile, low cost, and are easy to fabricate. The key idea is to place complementary split-ring resonators horizontally between the patch and the ground plane. Optimizing the split rings geometry leads to high levels of miniaturization. Ouedraogo et al. simulate three miniaturized patch antennas at 2.45 GHz and with different radii of 1.2, 0.8, and 0.6 cm to achieve 1/4, 1/9, and 1/16 of the traditional patch area respectively. Compared to traditional patch antennas, they achieve a size reduction of 75% with good impedance matching. This thus makes them suitable for use on pico-satellites. They, however, have smaller bandwidth; i.e., 1.2% (29.4 MHz), 0.8% (19.6 MHz) and 0.4% (9.8 MHz) and have a low gain because of their back loop pattern.

c: CYLINDRICAL SKIRTS WITH SHORTING PINS

The main advantage of wire patch antennas is their low profile, large bandwidth and monopolar type radiation pattern. However, their ground planes are generally too cumbersome as compared with the size of the radiating element [82]. In [31], Addaci et al. demonstrated a new design with a smaller, low profile circular wire patch antenna that operates in the 2.4-2.5 GHz; i.e., the ZigBee application frequency band [83]. The key idea is to bend the metallic plates of the upper and lower patches to form cylindrical skirts. The upper patch is a radiating element while the lower patch is a ground plane. These two patches are then connected using shorting pins. Moreover, the main advantage of upper and lower skirts is their ability to provide a better control of antenna performance in terms of resonant frequency and its overall dimension. Also, the distance between shorting wires and feeding pins allow the control of the antenna's operating frequency without changing its dimensions. They reported a miniaturization ratio of 42% and bandwidth of 4.7%. Compared to the patch antenna design in [34], the one in [31] has a wider bandwidth and higher front to back ratio.

d: ARTIFICIAL MAGNETIC CONDUCTOR

An Artificial Magnetic Conductor (AMC) is a structure with a distinct reflection phase property. Specifically, it introduces a zero degree reflection phase shift to incident waves [84]. To this end, Rahmadani et al. in [25] investigate to use this structure to miniaturize microstrip patch antennas. The main approach is to replace the antenna ground plane with an AMC structure, and thereby, acts as a virtual ground plane. This is important as it has good radiation patterns without unwanted ripples or side lobes and it reduces the antenna size by 31%. The main limitation is its low gain; i.e., 1.53 dB.

e: SHORTING PINS

Shorting pins help enhance patch antenna performance characteristics; i.e., bandwidth, as well as reduce their size [85]. Malekpoor and Jam [39] designed a small size E-shaped microstrip patch antenna. The main technique is to use two shorting pins between the edge of the upper patch (asymmetric E-shaped patch) and the ground plane. This increases the effective electrical length of the patch and reduces its physical size. Moreover, the use of shorting pins leads to a lower resonant frequency and wider bandwidth. The other approach is the use of an asymmetric E-shaped patch with unequal resonance arms to generate three resonant frequencies and hence achieve a wide bandwidth. Malekpour et al. reported a wide -10 dB bandwidth; i.e., 4110 MHz (3.34-7.45GHz), high peak gains; i.e., 5, 6.3 and 8 dB, and low return losses; i.e., -25, -28, and -22 dB at resonant frequencies of 4.74, 6.13 and 6.73 GHz respectively. Compared to the antenna designs in [25], [26], [31], and [34], the one in [39] has much wider bandwidth, provides higher gains, and is small; i.e., $3.4 \times 1.3 \times 0.7$ cm^3.

B. SLOT ANTENNAS

Fig. 3 shows a typical slot antenna that is normally made of an infinite conducting sheet (ground plane) that has a rectangular slot cut. The microstrip line is used to feed the slot antenna by applying a voltage across the slot. This generates an electrical field and currents within and around the slot. Slot antennas are cheap (low cost material), easy to fabricate, robust, have good radiation performance and have very small profile.

TABLE 5. Different slot antenna designs and their performance.

Reference	Gain (dB)	Size (cm)	Band (GHz)
Sievenpiper et al. [37]	4	6.3×6.3×0.03	S-band (2.34)
Razavi et al. [35]	4.8	3.7×1.61×0.078	X-band (8.8)
Row et al. [48]	4.5	11×10×0.22	L-Band A (1.67), B(1.77) and C (1.9)
Tu et al. [54]	12.45	16×17×0.68	S-band (2.45)
Liao et al. [27]	5	6×6×0.08	S-band (2.45 and 3.15)
Behdad et al. [29]	1.7	5.73×5.94×0.05	UHF-band (0.848, 0.85 & 0.86)
Row [36]	3.3	5.4×5.4×0.16	S-band (2.695)
Azadegan et al. [46]	4.5	10×8×0.0787	UHF-band (0.336) and L-band (1.3)
Wong et al. [43]	3.5	8×8×0.16	L-Ban (1.5) and (1.720)
Lee et al. [53]	3	10×10×0.16	L-band (1.58) and S-band (2.59)
Azadegan et al.[32]	3	5.5×5.5×0.0787	UHF-band (0.3)
Azadegan et al. [33]	2.7	5.327×5.327×0.05	UHF-band (0.337)
Ghosh et al. [52]	2.3	12×12×0.254	S-band (2.3 and 3.26)
Hong et al. [38]	3.7	5.3×4.6×0.685	S-band (2.25)

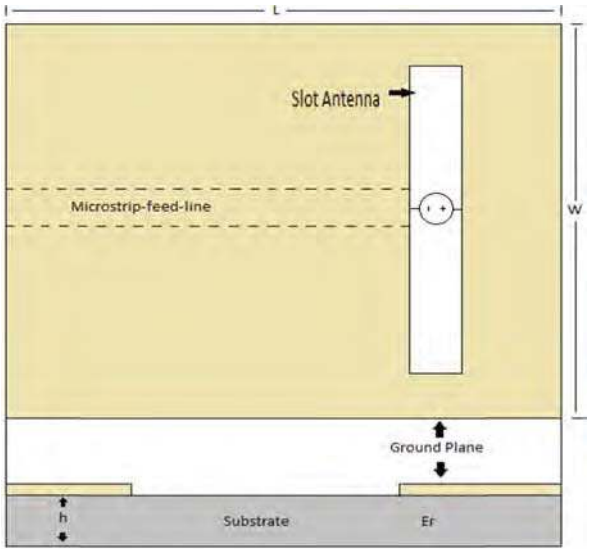

FIGURE 3. A rectangular slot antenna.

These advantages make slot antennas suitable for pico-satellite communications.

Here we review twelve slot antenna designs that aim to achieve beam steerability, high gains, small size, and wide bandwidth. As Table 5 shows, all these designs achieve gains ranging from 0.6 to 4.8 dB, with an antenna size ranging from $3.7 \times 1.61 \times 0.078\ cm^3$ to $12 \times 12 \times 0.254\ cm^3$. Moreover, they work in the UHF, L, S, C and X frequency bands (0.3 – 8.8 GHz). In terms of gain, bandwidth and size, all these designs are suitable for pico-satellites communications.

Different techniques and approaches are used in [27], [29], [32], [33], [35]–[38], [43], [46], [48], and [52]–[54] to enhance the radiation pattern of slot antennas, whilst reducing their size. The superior gain of 12.45 dB of miniaturized slot antennas reported in [54] leads to better and long distance communication between pico-satellites, and with a ground station. However, their main limitation is the narrow bandwidth and large antenna size; i.e., $16 \times 17 \times 0.68\ \text{cm}^3$. On the other hand, the design of [33] has a small antenna size; i.e., $5.327 \times 5.327 \times 0.05\text{cm}^3$, and a low gain of 2.7 dB. In terms of bandwidth, Liao and Chu [27] reported a significant enhancement in the CP bandwidth of 51.7% at the 2.45 and 3.15 GHz frequency bands, high gain of 5 dB and small antenna size; i.e., $6 \times 6 \times 0.08\ \text{cm}^3$. To date, the only design with steerability is the one reported in [48] where reconfigurable polarization is achieved using quasi-lumped quadrature coupler. Further details can be found in Section 2.2.1. In order to make the designs in [27], [28], [32], [33], [35]–[38], [43], [46], and [52]–[54] steerable, researchers have employed different techniques and approaches. For example, using arrays and external circuits. Next, we further discuss each work in more details.

1) STEERABILITY AND GAIN IMPROVEMENT

Beam-steering and high gain antennas are key components in applications that require tracking and frequent satellites repositioning. The main techniques used to achieve beam-steering and high gain include the cavity-backed model [37], half mode substrate integrated waveguide (HMSIW) [35], quasi-lumped quadrature coupler (QLQC) [48], and parasitic patch and windowed metallic superstrate [54].

a: CAVITY-BACKED MODEL

This is an important technique as it suppresses the back-lobe radiation of the antenna, and hence increases its directivity and gain [86]. In [37], Sievenpiper et al. describe the use of a cavity-backed model for a low-profile slot antenna that operates in the 2.34 GHz to achieve higher gain and better radiation performance. The key idea is to use a thin cavity-backed crossed-slot antenna with a single probe feeding network. The use of two orthogonal crossed-slots with slightly different lengths provides circular vertical polarization. This is important as it enhances the signal strength and reception; hence, it helps establish cross-links between satellites. Furthermore, this technique prevents back radiation. This in turn increases the antenna gain and facilitates long distance communications. They reported a gain of 4 dB for LP and CP.

The main limitation is the use of a quarter wave depth cavity that results in a non-negligible increase to the total antenna weight as the added cavity is of size $6.3 \times 6.3 \times 0.3$ cm^3.

b: HALF MODE SUBSTRATE INTEGRATED WAVEGUIDE

The main advantage of this technique is the reduction in microstrip patch antenna size whilst maintaining the same resonant frequency. In [35], Razavi et al. applied this technique to create a novel low-profile circularly polarized cavity-backed antenna for right and left hand polarization based on half mode substrate integrated waveguide technique [87]. The key idea is to use triangular quarter-wave length patches as a cavity. The resulting antenna has two electrical fields with equal magnitude and 90 degree phase shift. This is important as it achieves high gain and CP. Moreover, applying HMSIW to the cavity backed antenna design of [35] leads to a further reduction of the substrate integrated waveguide (SIW) that is used in conventional metallic cavity-backed antennas. They reported high gains of 4.87 and 4.2 dB for right and left hand CP. Compared to the design in [59], the one reported in [35] has a much smaller structure waveguide and hence smaller antenna size; i.e., $3.7 \times 1.61 \times 0.078$ cm^3, wider bandwidth; i.e., 1.74% (153 MHz) and similar gains of about 4.20 to 4.80 dB.

c: QUASI-LUMPED QUADRATURE COUPLER (QLQC)

This tuneable coupler has the ability to generate polarization diversity with frequency agility [88]. To this end, Row and Chuang-Jiashih [48] propose a novel design for a frequency agile slot antenna with reconfigurable polarization. This is an important capability as switching between circular and linear polarization at high gains leads to better signal strength. The main approach is to implement the ring slot antenna with a metallic reflector and then to excite it with a QLQC. The use of a reflector ensures the back radiation is reduced and hence, increases gain. Moreover, QLQC works in two different modes; quadrature hybrid mode and T-junction power divider mode to provide circular and linear polarizations respectively. They reported a high gain of 4.5 dB and a bandwidth of about 2.9% (1.77 GHz).

d: PARASITIC PATCH AND WINDOWED METALLIC SUPERSTRATE

This technique has the ability to increase antenna gain significantly. This is important for many applications that require high gains; e.g., point-to-point communications. In [54], Tu et al. present a novel low-profile, high gain slot antenna that operates in the 2.35 to 2.55 GHz band. The main approach is to print parasitic patches symmetrically to the feeding line. This changes the bi-directional radiation pattern to unidirectional and hence, increases slot antenna gain. In addition, placing a windowed metallic superstrate above the slot antenna leads to further gain enhancement. The main advantage is the superior gain of about 12.45 dB for long distance communications. Its main limitation is its large size; i.e., $16 \times 17 \times 0.6$ cm^3. Compared to the designs in [35], [37], and [48], the design in [54] has a much higher gain and provides longer communication distance.

2) ANTENNA BANDWIDTH ENHANCEMENT

The main techniques used to enhance bandwidth include using a coplanar waveguide (CPW) [27], inductive elements [29], series feed configuration [36], folded and self-complementary structures [46], asymmetry structure [43], and distributed and lump elements [53]. All these techniques achieve significant enhancement in bandwidth ranging from 2.1% (0.027 GHz) to 51% (1.5 GHz) and operate in the 0.336 to 3.15 GHz range. Moreover, these approaches have no significant effect on antenna size.

a: COPLANAR WAVEGUIDE (CPW) FEED

This feed mechanism is an alternative to using a microstrip-line because it has many advantages such as low dispersion, low radiation leakage, and the ability to effectively control the characteristic impedance of an antenna [89]–[91]. In [27], Liao et al. present a square slot antenna that has excellent broadband CP bandwidth. This is important for modern wireless communication as the signal level remains constant with varying antenna angles. This is required for a cross link communications between a transmitter and a receiver. The main approach is to feed the slot antenna with a lightening-shaped feed-line from the centre signal strip of the feeding CPW, and then to embed a tuning stub in the feeding. Moreover, Liao and Chu [27] embed two symmetrical F-shaped slits in the opposite corners of the ground plane to introduce more resonant branches. They reported a superior bandwidth of 51.7% at the 2.45 and 3.15 GHz frequency bands. It, however, suffers from back-lobe radiation which in turn reduces gain.

b: SERIES INDUCTIVE ELEMENTS

Behdad and Sarabandi [29] presented a small antenna with a wide bandwidth. This is important as it leads to better communication performance and coverage, less fabrication cost, and thus is more suitable for pico-satellites. The key idea is to examine the use of multi-resonance (double resonant) antenna structures at 850 MHz and inductively loaded miniaturized slot antenna at 1 GHz. The use of series inductive elements along the antenna slot leads to a reduction in the guided wavelength of the resonant slot line. This in turn decreases the overall antenna length. In addition, using a double resonant antenna leads to significant bandwidth enhancement. As a result of using a single slot antenna (SEA), the antenna has a bandwidth of 0.9% (8 MHz) while 2.54% (21.6 MHz) for a double slot antenna (DEA). This is an improvement of about 1.64%. Behdad and Sarabandi [29] remarked that the only limitation is the need for an external network for impedance matching.

c: SERIES FEED CONFIGURATION

This configuration is mainly used to improve CP bandwidth. In [36], Row presents a CP squarer-ring slot antenna design that operates in the 2.695 GHz and has a small size and

wide bandwidth. The main approach is to feed the narrow square-ring slot antenna with a series microstrip-line-feed configuration. They use a coupling strip to feed the two orthogonal sides of a square ring slot antenna with the same amplitude at 90 degree out of phase by optimizing slot side lengths. This is important as it achieves CP without the need to use an external coupler, which in turn enhances bandwidth and reduces antenna size. Moreover, Row uses a microstrip impedance transformer to achieve good impedance matching at 50 ohm. He reports a CP bandwidth of 6.1% (2.695 GHz) at a return loss of about −30 dB. Compared to the designs in [27] and [29], the antenna in [36] has wider bandwidth. Its main limitation is its back-lobe radiation, which decreases gain.

d: FOLDED AND SELF-COMPLEMENTARY STRUCTURES

Folded and self-complementary structures approaches are mainly used to increase the bandwidth of miniaturized antennas. Azadegan and Sarabandi [46] employ such structures to increase bandwidth. Their first approach is to use a complementary pair of miniaturized slot antennas; i.e., a miniaturized folded printed wire. The main idea is to increase the radiating aperture of the antenna without increasing the total antenna size or reducing its efficiency. Additionally, replacing slot lines by metallic strips to work as a ground plane leads to wider bandwidth of about 0.60% (0.336 GHz). The second approach is to implement a self-complementary folded antenna structure. This approach is a combination of the first approach and a normal folded slot antenna. Furthermore, its final structure is a self-complementary H-shaped antenna with a wide bandwidth of 2.1% (1.3 GHz). Azadegan and Sarabandi [46] pointed out that this design can be matched easily without the need for external matching networks. This is important as it leads to less complex and low cost designs.

e: ASYMMETRY STRUCTURE

This technique is simple and is mainly used for CP bandwidth enhancement. In [43], Wong et al. propose a square and annular printed ring antenna that achieves 3dB axial ratio CP bandwidth and operates in the 1.5 and 1.720 GHz band. This is significant as CP is important for establishing cross-link communications. Moreover, achieving wider bandwidth and higher gain means better and longer communication distance between any two satellites. The key idea is to introduce some asymmetry into the structure of the ring slot antenna in order to enhance its bandwidth and to obtain good CP. The resulting design achieves a higher bandwidth of 4.3% (0.0645 GHz) while for an annular ring slot antenna it is 3.5% (0.0602 GHz). The main limitation is the slight asymmetry in radiation patterns. The authors posit that this is due to the asymmetry inherent in the antenna structure.

f: DISTRIBUTED AND LUMP ELEMENTS

This technique enhances bandwidth by varying the CP antenna frequency. Lee and Row [53] propose a lightweight annular-ring slot antenna that operates in the 1.58 and 2.59 GHz bands. The main approach to obtain CP is to excite the square ring slot antenna using a L-shaped coupling strip. This provides good CP bandwidth and has a stable radiation pattern across all supported bandwidth. Moreover, distributed and lump elements are used to vary the CP operating frequency to enhance its bandwidth. The reconfigurability of the operating frequency is important as it leads to better CP performance. Compared to the designs in [29], [36], [43], and [46], the antenna design in [53] has wider bandwidth; i.e., 730 MHz. However, the main limitation of the design in [53] is its large size; i.e., $10 \times 10 \times 0.16$ cm^3.

3) SLOT ANTENNA MINIATURIZATION

As mentioned in Section 1, pico-satellites are limited in size and are light. This means antenna size is very important. To this end, miniaturization is critical. In this respect, the main techniques include inductive load [32], physical aperture expansion [33], loading wires [52], and series parallel lines [38]. These techniques are capable of yielding reduction ranging from $3.7 \times 1.61 \times 0.078$ (smallest) to $16 \times 17 \times 0.68$ cm^3 (largest).

a: INDUCTIVE LOAD

This technique is mainly used to miniaturize an antenna and enhance its bandwidth. The approach involves loading the antenna with series inductive elements (coiled wire) along the aperture of the slot antenna. In [32], Azadegan et al. present a novel small slot antenna that works in the 0.3 GHz frequency band. The main approach is to short the slot line with an inductor; the line has an electrical length is less than a quarter wavelength. Moreover, they use a substrate with rectangular spiral geometry. This is important as it leads to higher antenna efficiency. The main limitation, as pointed out by the authors, is the resulting narrow bandwidth; i.e., 1.6% (4.8 MHz). This is because a higher inductive load leads to a reduction in bandwidth. Another limitation is the dramatic increase in dielectric and ohmic losses [92] that are attributed to the concentration of fields over a very small area of substrate. An open problem is how to increase gain and bandwidth without increasing physical size and loss.

b: PHYSICAL APERTURE EXPANSION

This is an effective technique that expands the physical size of an antenna's slot to enhance bandwidth and to achieve high efficiency without increasing antenna size. Azadegan and Sarabandi [33] propose a new miniaturized antenna structure with a large radiation conductance (physical aperture), bandwidth, and efficiency as compared to the miniaturized slot antenna presented in [32]. Advantageously, the resulting antenna has the same size. This is important as it leads to high communication performance, and less fabrication cost. The key idea is to increase only the physical aperture of the folded slot to as large as that of the miniaturized slot in the design of [32]. This increases the bandwidth and the efficiency of the folded slot antenna without increasing its overall size. Moreover, they use

a coplanar waveguide. This significantly reduces matching impedance but the resulting antenna has a low gain.

c: LOADING WIRES

The main advantage of this technique is its ability to reduce the operating frequency without increasing antenna length. In [52], Ghosh et al. present a new miniaturization technique for planar slot antennas using loading wires. These wires are used on either sides of the antenna aperture and they penetrate the substrate or a cavity backing to compensate for the reactive environment. This is important as it leads to a reduction in resonant frequencies without increasing antenna size. The authors propose two slot antenna prototypes; a slot antenna on a dialectic substrate that operates in the 2.32 GHz band, and a slot antenna on a ground plane with backing cavity that operates in the 3.26 GHz band. A reduction of 28.83% in resonant frequency is achieved for a slot antenna on a dielectric substrate, and 45.52% for a slot antenna on the ground plane. Moreover, the use of backing cavity suppresses back radiation, and improves gain.

d: SERIES OF PARALLEL STRIP LINES

This technique is mainly used as an alternative to the traditional cavity-backed model. Hong *et al.* [38] outline a new technique to reduce the size of cavity-backed slot antennas (CBSA) by substituting the traditional cavity structure with a series of miniaturized transmission line type resonators. The main idea is to design the slot antenna using a finite width metallic strip connected to a number of parallel short-circuited microstrip lines that have the same physical and electrical length as the width of the ground plane. This reduces the physical length of microstrip lines while retaining their electrical length. They achieve a size reduction of approximately 65%. Furthermore, despite its reduced physical dimensions, the antenna has a gain of 3.7 dB with excellent impedance matching, and high radiation efficiency.

III. QUALITATIVE EVALUATION

We now provide a qualitative comparison of planar antenna designs and their suitability for use on pico-satellites. Table 6 summarizes their features and performance in terms of mass, size, gain, beam steerability, type of polarization, operating frequency band, and return loss. Most designs are relatively small, light, have small return loss and provide CP. Amongst all antenna designs listed in Table 6, only the designs in [40], [44], [45], [47], [49], and [37] have steering capability. On the other hand, non-steerable designs require external circuits and arrays in order to become steerable; this, however, adds extra cost and complexity to the design. Moreover, the design in [49] achieves the highest gain of 18 dB at a wide bandwidth of 47.8% (2.95 GHz); however, its size is very large, i.e., exceeds 10 cm, and is not suitable for pico-satellites. In terms of bandwidth, the designs of [28] and [39] demonstrate a significant bandwidth enhancement of 98% (3.57-10.46 GHz) and 76.18% (3.43-7.45 GHz) respectively. As set out in Table 6, we use the following criteria to determine the most suitable antenna designs for use on pico-satellites: small physical size at the lower end of operating frequencies, wide bandwidth, small return loss (<-10 dB), steerability and relatively high gain. The most important factor is antenna size. The best designs that address most of the pico-satellite's challenges are to be found in [27], [28], and [39]. They achieve wide bandwidth, are small and have high gains at lower end of operating frequencies. Their main limitation is their lack of steering capability. In the next section, we will evaluate [27], [28], and [39] on a common platform.

IV. QUANTITATIVE EVALUATION

As mentioned in Section 3, the designs of [27], [28], and [39] address the most pico-satellite challenges listed in Table 2 and provide good radiation performance as compared to all reviewed planar antenna designs. However, their performance in the presence of a satellite body is unknown. To this end, we employ the High Frequency Structure Simulator (HFSS) version 16 [93] to study their performance in terms of return losses, gains, bandwidth, and axial ratios when operating on a 2U CubeSat.

We first present the CPW-feed square, shorted patch, and asymmetric E-shaped microstrip patch antenna designs. Then we present and compare the results of each antenna design with and without the effect of the 2U (10cm $\times$ 10cm $\times$ 20cm) CubeSat body. Lastly, we comment on their suitability for CubeSat communications.

A. CPW-FEED SQUARE SLOT ANTENNA [27]

Fig. 4(a) shows the square slot antenna model used in our evaluation. The antenna has a total size of 60 $\times$ 60 mm^2; it is fabricated on a FR4 substrate that is 0.8 mm thick. The Coplanar Wave Guide (CPW) feed line technique is used with a fixed width of a single strip; i.e., 4.2 mm and the gap between the line and ground plane is 0.3 mm in length in order to achieve 50 Ω matching. To enlarge the CP bandwidth, the ground plane has two symmetrical F-shaped slits. This CP bandwidth can be further enhanced by varying the dimensions of the lightening-shaped feedline. The evaluated antenna operates at resonant frequencies of 2.45 and 3.2 GHz; see Fig.7. We see that the obtained resonant frequency 3.2 GHz is slightly lower than the resonant frequency obtained by the authors of [27], i.e., 3.45 GHz. This margin of error is acceptable as both frequencies are located within the operating -10 dB bandwidth 2.3 to 3.8 GHz. To observe the effect of the satellite body on the antenna's performance, the CPW-feed square slot antenna is mounted on the 2U CubeSat face; see Fig. 4(b).

B. SHORTED PATCH ANTENNA USING FOLDED-PATCH TECHNIQUES [28]

Fig. 5 (a) shows the tested shorted patch antenna model. The upper and lower patches have dimensions 18 $\times$ 15 and 7.5 $\times$ 6.5 mm^2 respectively. These patches are connected

TABLE 6. Comparison between all types of planar antennas.

Ref	Method	Gain (dB)	Volume (cm^3)	Mass	Beam Steerability and type	Polarization & Bandwidth (BW)	Freq. (GHz)	Return Loss (dB)	Suitability for pico-sats
[47]	Sequential phase-rotation	6.9	9 × 9 × 0.5	162g	Electronic pointing using Digital phase shifter	CP	5.8	-25	✓
[44]	Sequential phase-rotation	7.1 CP and 7.5 LP	15×15 × 0.96	Light	Electrically steerable	CP or LP BW= 3.4%	2.37	-35	×
[49]	Sequential phase-rotation	18	16 × 16 × 0. 35	Light	Electrically steerable	CP BW=47.8% with AR<1 dB	6.175	-27	×
[45]	Retrodirective (self-steering)	6.25	10×10× 0.16	Light	Self-Steering	CP	10.5	n/a	✓
[40]	Beam forming algorithm	4.8	10×10×0.16	heavy	Electrically steerable	CP	2.45	n/a	✓
[50]	Photonic band-gap (PBG) structures	5.02	12×16.8× 2. 5	Light	Not steerable	Cross polarization. BW = 5.4 %	14.15	-12	×
[51]	Transparent mesh line geometry	n/a	8.01×8.01× 2.25	Light	Not steerable	CP BW= 80 MHz	2.40	-20	✓
[42]	Single proximity coupled feed	6	7 ×7 × 0.16	Light	Not steerable	CP	1.525	-40	✓
[24]	Agile polarization	4 CP and 6.2 LP	2.77×2.77×0 .0892	Light	Not steerable	CP or LP BW= 3.8%	3.5	-34	✓
[41]	Cavity model	5.9	8.8 × 8.8 × 2.5	Light	Not steerable	CP	4.32	-12	✓
[23]	U-slot and L-slit geometries	U-slot 2.58 L-slit 2.4	U-Slot ≈ 5.4 × 5.4× 0.7 L-Slit ≈ 4 × 4× 0.7	Light	Not steerable	CP U-slot BW= 53.54% L-slit BW= 45.12%	U-slot 4.5 L-slit 5.5	U-slot -15.04 L-slit -24.29	✓
[28]	Folded-patch feed	1st 4.9 2nd 3.9	1st design 2.8 × 1 × 0.7 2nd design 1.8 × 1.5 × 0.7	Light	Not steerable	CP 1st design BW= 94.17% 2nd design BW= 98.22%	1st 5 2nd 4.2	1st -23.69 2nd -34.15	✓
[26]	Meandering	n/a	2.21× 2.21 × 1.5	Light	Not steerable	CP 1st design BW= 2.98% 2nd design BW= 1.15%	1st 1.575 2nd 0.869	1st -28 2nd -30.5	✓
[34]	Meta-material	5.96, 4.86, & 4.23	3.14 × r^2 × 0.078 r =1.2, 0.8, and 0.6 cm	Light	Not steerable	Cross polarization	2.45	-26	✓
[31]	Cylindrical skirts with shorting pins	n/a	3.14 × 2.7^2 × 1.37	Light	Not steerable	Cross polarization BW=4.7% (116.34 MHz)	2.45	-30.5	✓
[30]	Sequential phase-rotation	5.9	3.97×1.2×0. 20	Light	Not steerable	CP BW= (1500MHz)	2.45	-25	✓

TABLE 6. (Continued) Comparison between all types of planar antennas.

[25]	Artificial magnetic conductor	1.53	3.8×3.8×0.32	Light	Not steerable	CP, BW= 4.08% (100 MHz)	2.45	-13	✓
[37]	Cavity-backed model	4	6.3 × 6.3 × 0.03	Light	Steerable	CP	2.34	-12	✓
[35]	Half mode substrate integrated waveguide	RHCP 4.8 LHCP 4.20	3.7 × 1.61 × 0.078	Light	Not steerable	CP RHCP, BW= 1.74 %, LHCP, BW= 0.66%	RHCP 8.67 LHCP 8.67	RHCP -33 LHCP -20	✓
[48]	Quasi-lumped quadrature coupler	CP 4.5 LP 4	11 × 10 × 0.22	Light	Not steerable	CP or LP	CP 1.67 LP 1.9	CP -23 LP -16.5	✓
[54]	Parasitic patch and windowed metallic superstrate	12.45	16×17×0.68	Light	Not steerable	CP BW= 80 MHz	(2.45)	-15	×
[27]	Coplanar waveguide (CPW) feed	5	6 × 6 × 0.08	Light	Not steerable	CP BW= 1500 MHz	3.45	-17	✓
[29]	Series inductive elements	1.7	5.73 × 5.94 × 0.05	Light	Not steerable	CP BW= 21 MHz	0.848	-35	✓
[36]	Series feed configuration	3.3	5.4× 5.4 × 0.16	Light	Not steerable	CP, BW=6.1%	2.695	-34	✓
[46]	Folded and self-complementary structures	1st 4.5 2nd 1.3	1st 10 × 8× 0.0787 2nd 4×4×0.0787	Light	Not steerable	Cross polarization BW=1.1-2.1 %	1st 0.336 2nd 1.3	1st -26.5 2nd -28	✓ ✓
[43]	Asymmetry structure	3.8	8 × 8 × 0.16	Light	Not steerable	CP	1.720	n/a	
[53]	Distributed and lump elements	3	10 × 10 × 0.16	Light	Not steerable	CP	1.58	-10	✓
[32]	Inductive Load	3	5.5 × 5.5 × 0.0787	Light	Not steerable	Cross polarization	0.3	-25	✓
[33]	Physical aperture expansion	2.7	5.327×5.327 × 0.05	Light	Not steerable	Cross polarization	0.337	-30	✓
[52]	Loading wires	2.3	12×12×0.254	Light	Not steerable	Cross polarization	3.26	-18	×
[38]	Series of parallel strip lines	3.7	5.3×4.6×0.685	Light	Not steerable	CP	2.25	-30	✓
[39]	Shorting Pins	5, 6.3 and 8	3.4×1.4×0.7	Light	Not steerable	n/a	4.74, 6.13 and 6.73	-24, -28.5, and -22	✓

together via a folded ramp-shaped part. Also, they are connected to a 30 × 30 mm^2 ground plane through shorting pins and probe feed. Moreover, in order to obtain wider bandwidth, air substrate and folded ramp-shaped part are used to decrease the quality factor (Q) and inductive reactance of the probe feed. The main purpose of using shorting pins at the edges of the upper patch is to achieve miniaturization at wide impedance bandwidth. In addition, the centre pin on the upper patch is used to broaden the impedance bandwidth by generating resonances at 4.45 and 7 GHz. Fig. 5 shows the shorted patch antenna on a 2U CubeSat.

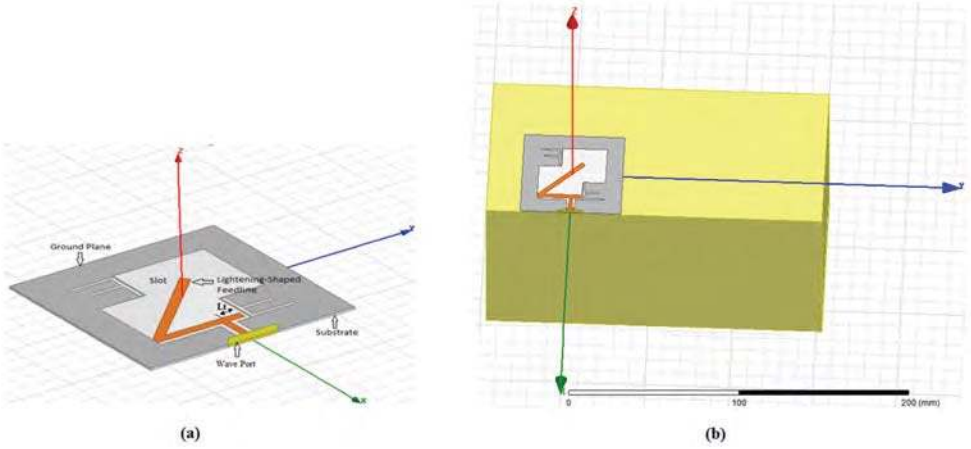

FIGURE 4. A CPW-feed square slot antenna: (a) geometry, and (b) installation on a 2U CubeSat face.

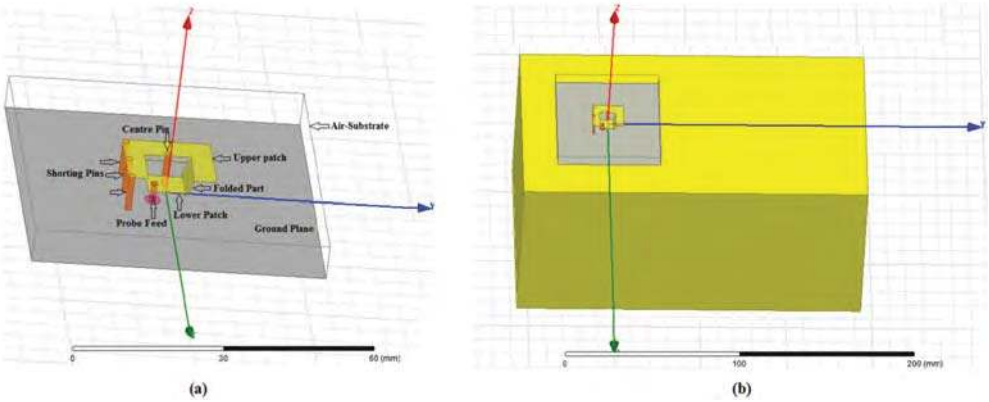

FIGURE 5. Geometry of a shorted patch antenna (a) without CubeSat, and (b) with CubeSat.

C. MINIATURIZED ASYMMETRIC E-SHAPED MICROSTRIP PATCH ANTENNA WITH FOLDED-PATCH FEED [39]

Fig. 6(a) shows a 3D model of a miniaturized asymmetric E-shaped microstrip patch antenna. The upper patch resembles an asymmetric 'E' with a total size of 34×13 mm^2. The folded-patch feed or lower patch has a rectangular shape with size 23×5 mm^2. The upper and lower patches are connected to the ground plane through shorting pins. Air is assumed to be the supporting substrate. The shorting pins are used to decrease the physical antenna size by increasing its electrical length. Moreover, the unequal arms of the asymmetric E-shaped patch (upper patch) are designed to produce three different resonant frequencies to enlarge the antenna's bandwidth. Fig. 6 (b) shows our implementation on the 2U CubeSat body.

D. SIMULATION RESULTS

1) CPW-FEED SQUARE SLOT ANTENNA

Fig. 7 shows the return losses over varying frequencies for the CPW-feed square slot antenna with and without the effect of the CubeSat body. We see that the CubeSat body has a significant effect on the return loss; we recorded increases from -27.5 to -10 dB. This means most of the power is reflected back to the antenna instead of being radiated into the space. Moreover, the operating frequency increases from 3.2 to 4.1 GHz. As shown in Fig. 7, the -10 dB bandwidth without CubeSat is 1600 MHz (2.3-3.9 GHz).

Fig. 8 shows the axial ratio of the CPW-feed square slot antenna with and without the effect of the 2U CubeSat body. Without the CubeSat, the antenna achieved a wide 3 dB axial ratio bandwidth of about 1120 MHz, ranging from 2.28 to 3.4 GHz. The CubeSat's surface has a significant effect on the axial ratio. In particular, placing the CPW-feed square slot antenna on the 2U CubeSat body reduces the 3 dB axial ratio bandwidth from 1120 MHz (without CubeSat) to 174 MHz (with CubeSat).

Fig. 9 presents the peak gain of the CPW-fed square slot antenna. For the with CubeSat case, the antenna achieves a gain of about 1.4 dB at 3.2 GHz. The maximum gains with and without the effect of the CubeSat body are 2.7 and -5 dB respectively at frequencies of 3.6 and 3 GHz

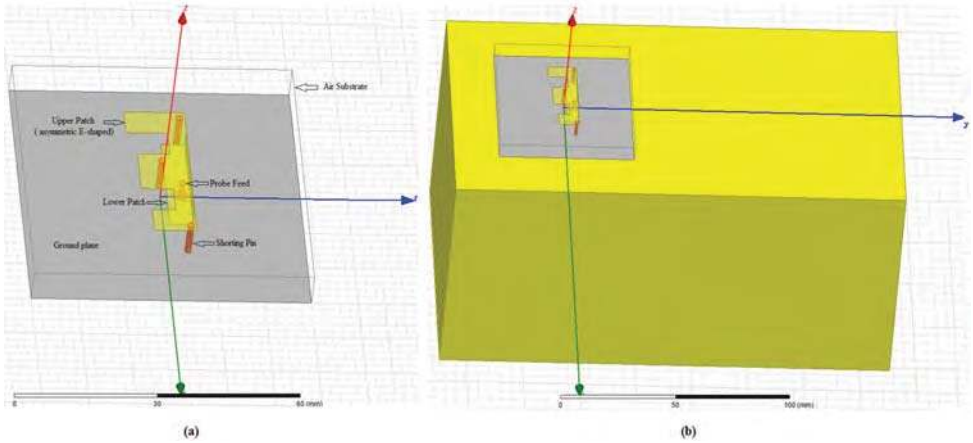

FIGURE 6. Geometry of an asymmetric E-shaped patch antenna (a) without a 2U CubeSat, and (b) with a 2U CubeSat.

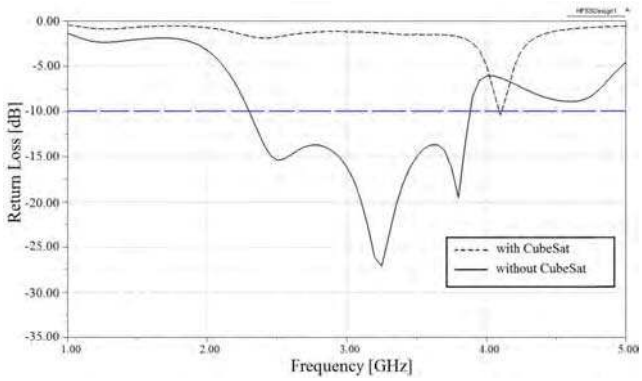

FIGURE 7. Return losses (S_{11}) of a CPW-feed square slot antenna.

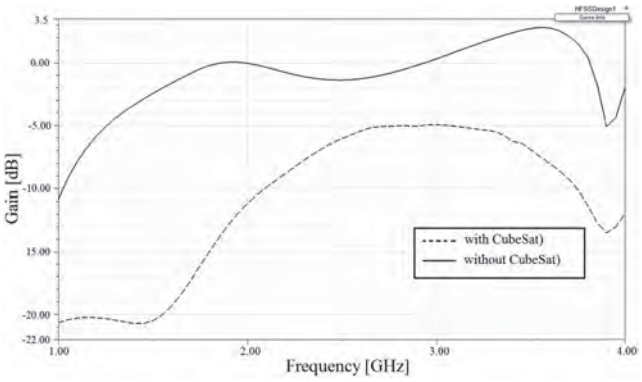

FIGURE 9. 2D gain of a CPW-feed square slot antenna.

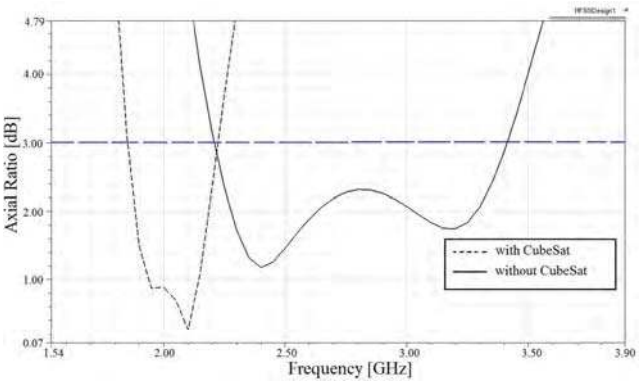

FIGURE 8. The axial ratio of the CPW-feed square slot antenna.

respectively; see Fig. 9. The 3D gains at 3.2 GHz are shown in Fig. 10 (a) and (b). We see that for the CubeSat case, the antenna has a higher gain.

2) SHORTED PATCH ANTENNA

Fig. 11 depicts the return losses of the shorted patch antenna with and without the effect of a CubeSat body. We see that the satellite body has a significant effect on the return loss; we observe decreases (or improvements) from −26.5 to −43.3 dB. This means more power is radiated into space and less power is reflected. Moreover, there is a slight shift of 0.2 GHz in the first resonant frequency and 0.5 in the second resonant frequency. Compared to the shorted patch antenna without CubeSat, the shorted patch antenna with CubeSat has less bandwidth; i.e., 7150 MHz and much smaller return loss; i.e., −43.3 dB at 4.3 GHz; see Fig. 11.

We now study the effect of a 2U CubeSat body on the axial ratio and gain of the shorted patch antenna. Fig. 12 shows the simulated axial ratio of the shorted patch antenna with and without a CubeSat as a function of frequency. We see that the axial ratio for the CubeSat case has a smaller CP bandwidth; i.e., 650 MHz. The CubeSat body also has a significant effect on the shorted patch antenna gain. Without the CubeSat, the gain increased by 2.1 dB over the 2-4.5 GHz frequency range and decreased by 1 dB over the 5.2-9 GHz range when the antenna is placed on the 2U CubeSat; see Fig. 13. The peak gain of the shorted patch antenna with and without a CubeSat is 4 and 6.2 dB respectively at 4.3 GHz. This is because the Aluminium surface of the CubeSat reflects some of the back lobe radiation forward. Hence, this yields further improvement in gain.

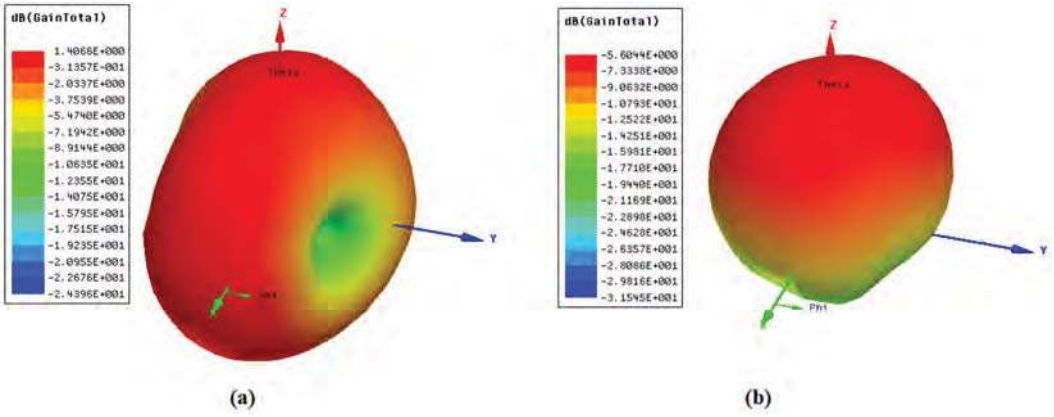

FIGURE 10. 3D gain of a CPW-feed square slot antenna at 3.2 GHz: (a) without, and (b) with CubeSat.

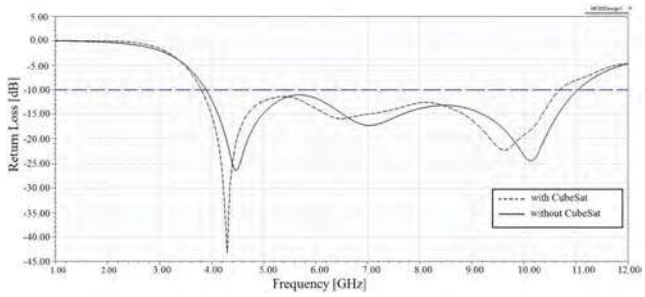

FIGURE 11. Return loss (S_{11}) of the tested shorted patch antenna.

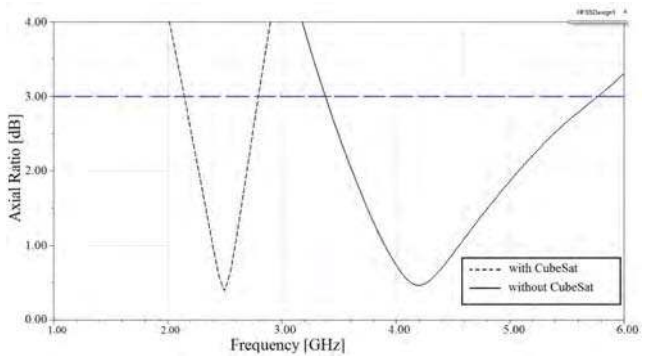

FIGURE 12. The axial ratio of the shorted patch antenna.

Fig. 14 shows a 3-D plot of the shorted patch antenna far field radiation pattern. Without the CubeSat, the antenna has a maximum gain of 4.0 dB as compared to 6.22 dB when used on the CubeSat. The radiation pattern of the shorted patch antenna for the without CubeSat case is uniform. In contrast, it is non-uniform and maximum gain is not at the broadside direction (Z direction) when the antenna is used on a CubeSat.

3) ASYMMETRIC E-SHAPED PATCH ANTENNA

Fig. 15 shows the simulated return losses of the asymmetric E-shaped patch antenna with and without the effect of the CubeSat body. We see that for both tested cases, the antenna has a similar resonant frequency of 6.5 GHz. When the antenna operates on the CubeSat, we see that it has a wide impedance bandwidth; i.e., 2300 MHz. On the CubeSat body, its bandwidth increased by about 100 MHz. Also, the return loss at the resonant frequency of 6.5 GHz decreases (or improves) slightly from −14 to −15.2 dB.

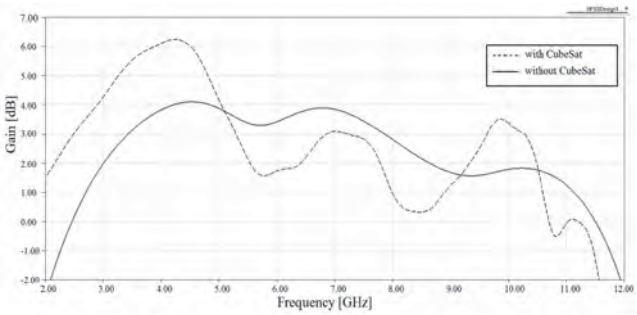

FIGURE 13. 2D gain of tested shorted patch antenna.

Fig. 16 shows the simulated axial ratio of the asymmetric E-shaped patch antenna with and without the effect of the 2U CubeSat body. On the CubeSat, the antenna's axial ratios are 0.9, 0.15 and 1.85 dB at frequencies of 2.3, 5.35 and 6.3 GHz, respectively. The achieved 3-dB axial ratio bandwidths are 200 MHz (2.2-2.4 GHz) and 1400 MHz (5-6.4 GHz). Without the CubeSat case, the asymmetric E-shaped patch antenna has an axial ratio of 3.07 dB at 5.15 GHz. This means the CubeSat body causes axial ratios of less than 3 dB and enlarges the 3-dB axial ratio bandwidth; i.e., 1400 MHz (5-6.4 GHz).

Fig. 17 shows the gain of the asymmetric E-shaped patch antenna versus varying frequencies. We see that the CubeSat body affects the E-shaped patch antenna by increasing its gain over the frequency range of 3 to 6.7 GHz and decreasing its gain for frequency ranging from 6.7 to 9 GHz. The gain of the antenna at resonant frequencies of 4.6 and 6.5 GHz is increased by 0.8 dB when used on the CubeSat; see Fig. 17. The peak gain of the E-shaped patch antenna on the 2U CubeSat is 8.4 dB at a resonant frequency of 5.8 GHz.

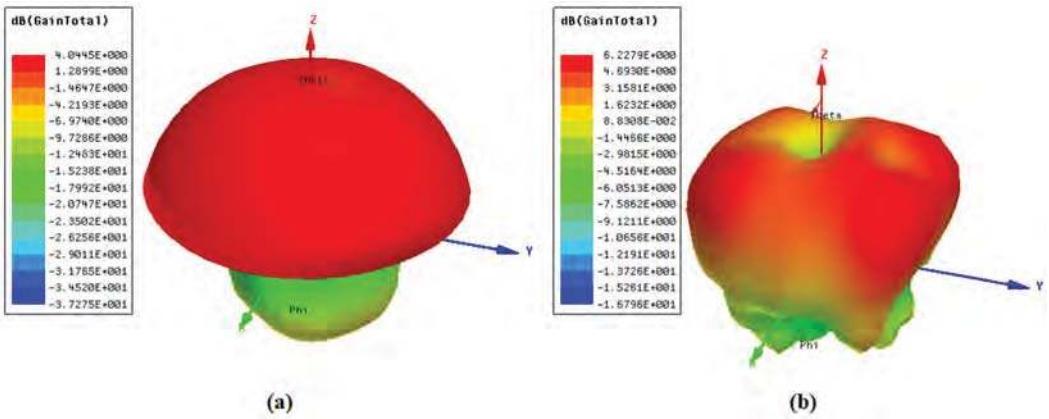

FIGURE 14. 3D gain of the tested shorted patch antenna at 4.3 GHz: (a) without, and (b) with CubeSat.

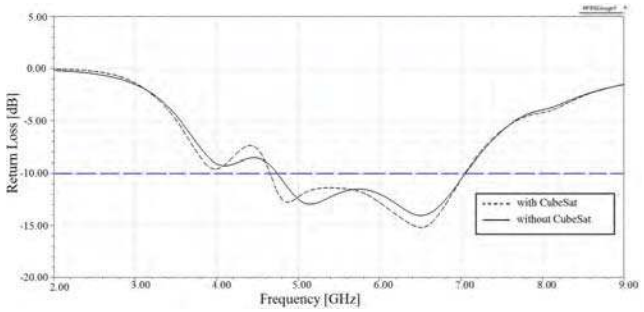

FIGURE 15. Return losses (S_{11}) of the asymmetric E-shaped patch antenna.

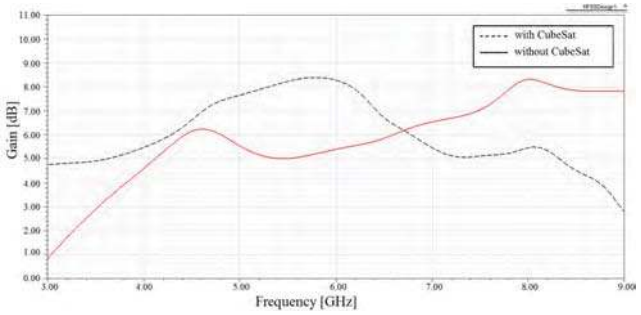

FIGURE 17. 2D gain of asymmetric E-shaped patch antenna.

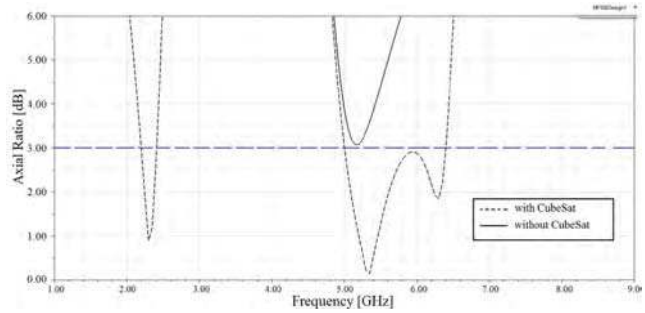

FIGURE 16. The axial ratio of the tested asymmetric E-shaped patch antenna.

Fig. 18 illustrates the simulated 3D gains of the asymmetric E-shaped patch antenna with and without the 2U CubeSat body at 4.75 GHz. Compared to the without CubeSat case, the antenna with CubeSat has a higher 3D gain; i.e., 7.3 dB. However, the radiation pattern of the antenna with CubeSat is non-uniform.

E. COMPARISON OF ALL THREE DESIGNS

We now provide a comparison between the three antenna designs. In particular, we compare the effects of a 2U CubeSat body on their return losses, axial ratios and gains. Fig. 19 plots the return losses of the shorted patch, asymmetric E-shaped microstrip patch and CPW-feed square slot antennas. Compared to the asymmetric E-shaped patch antenna and CPW-feed square slot antenna, the shorted patch antenna has smaller return loss; i.e., −43.3 dB at 4.3 GHz, and a much wider −10 dB bandwidth; i.e., 6900 MHz (3.8-10.7 GHz). In terms of resonant frequency, only the shorted patch antenna operates close to the S-band (2-4 GHz) with a resonant frequency of 4.3 GHz (with CubeSat); see Fig. 19. However, this resonant frequency; i.e., 4.3 GHz, does not belong to the 2.4-2.5 GHz unlicensed Industrial, Scientific and Medical (ISM) band, which is preferred for CubeSat communications. Therefore, the operating frequency of the shorted patch antenna needs to be shifted to 2.45 GHz. Moreover, we see that the CPW-feed square slot antenna has very high return loss when used on a CubeSat; i.e., −10 dB and a small non-uniform bi-directional radiation pattern. This is because the attached side of the antenna is not a ground plane and hence the satellite body acts as a ground plane and significantly affects the antenna's performance. One solution is to insert a PVC plastic sheet between the antenna and the CubeSat body [94]. Another solution is to keep some distance (air gap) between the antenna and the satellite body. This gap should be set such that there is no capacitance between the dielectric and the CubeSat body. Consequently, the satellite body will act as a reflector, and leads to higher gains.

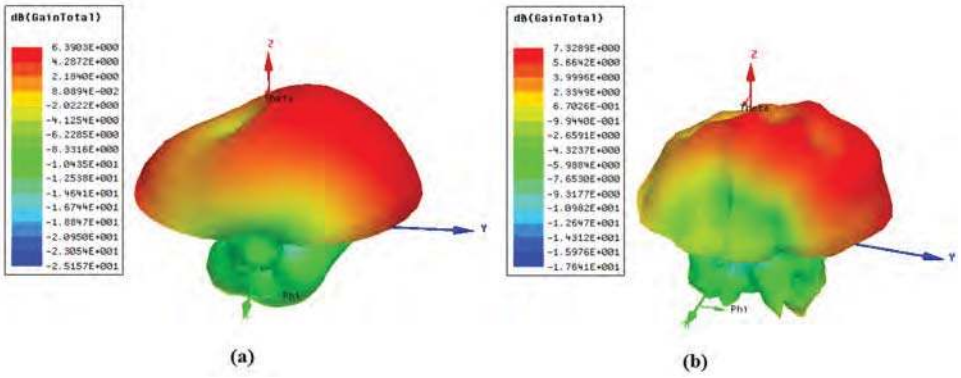

FIGURE 18. 3D gain of asymmetric E-shaped patch antenna at 4.75 GHz: (a) without, and (b) with CubeSat.

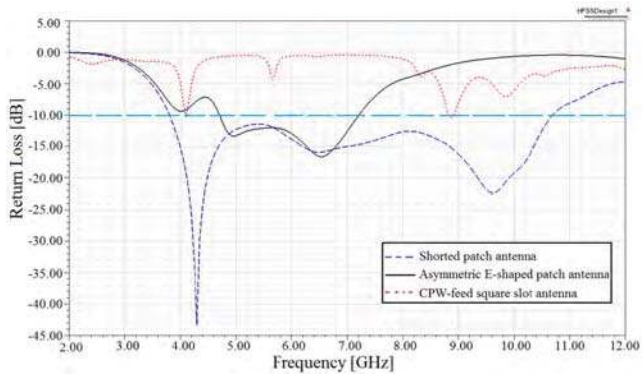

FIGURE 19. Return losses of the shorted patch, asymmetric E-shaped patch and CPW-feed square slot antennas on a 2U CubeSat body.

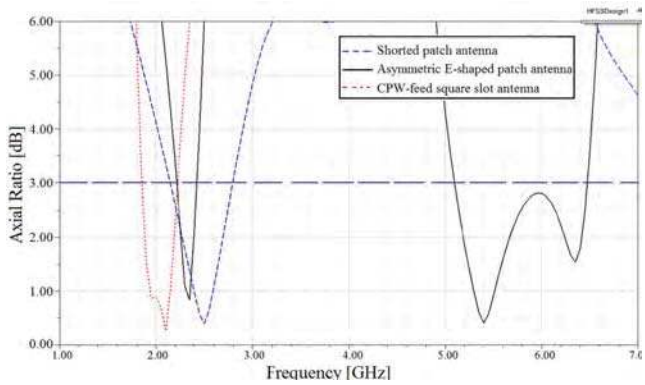

FIGURE 20. The axial ratio of the shorted patch, asymmetric E-shaped patch and CPW-feed square slot antennas on a 2U CubeSat body.

Fig. 20 shows the axial ratios of the shorted patch, asymmetric E-shaped microstrip patch and CPW-feed square slot antennas. All three antennas have an axial ratio less than 3 dB at different operating frequencies. Compared to the shorted patch and CPW-feed square slot antennas, the asymmetric E-shaped patch microstrip patch antenna has a wider 3 dB axial ratio bandwidth; i.e., 1400 MHz, and a smaller axial ratio; i.e., 0.14 dB. In the S-band frequencies (2-4GHz), the shorted patch antenna has

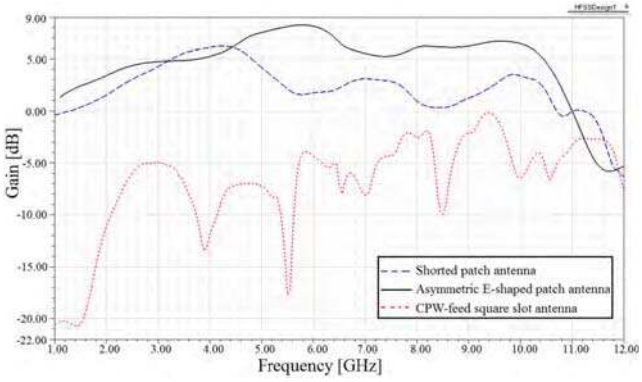

FIGURE 21. A comparison of gain of the tested shorted patch, asymmetric E-shaped patch and CPW-feed square slot antennas on a 2U CubeSat body.

a wider 3 dB axial ratio bandwidth than that of asymmetric E-shaped patch and CPW-feed square slot antennas; see Fig. 20. In terms of gain, the asymmetric E-shaped patch antenna has the highest peak gain of 8.39 dB at 5.8 GHz as compared to shorted patch and CPW-feed square slot antennas; see Fig. 21. The peak gain of the shorted patch, asymmetric E-shaped microstrip patch and CPW-feed square slot antennas in the 2.4-2.45 GHz band is 3, 4.4 and −6.3 dB, respectively. Further improvement in gain is needed for CPW-feed square slot antenna if it is to be used on pico-satellites.

The simulated radiation patterns of all three antennas on two planes (*xz*: $\varphi = 0°$ *and* *yz*: $\varphi = 90°$) are illustrated in Fig. 22. We see that their radiation patterns are rather symmetric in the xz and yz planes. The maximum radiation of the E-shaped patch and CPW-feed square slot antennas occur exactly at the boresight direction ($\theta = 0°$). Compared to CPW-feed square slot and shorted patch antennas, the E-shaped microstrip patch antenna has the widest Half Power Beamwidth (HPBW); e.g., 76° (xz-plane), and the highest peak gain at its boresight direction; e.g., 5.17 dB.

Table 7 compares all three candidate antennas in terms of volume, gain, bandwidth, return loss, robustness, beam

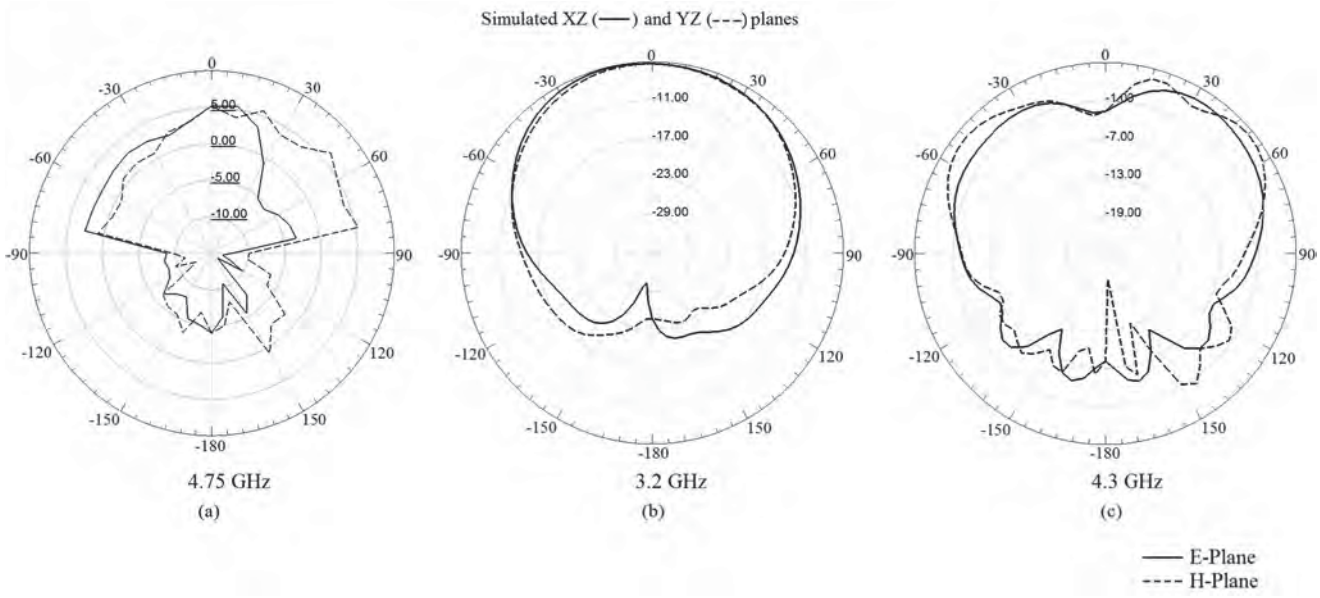

FIGURE 22. Simulated radiation patterns of an (a) E-shaped patch, (b) CPW-feed square slot, and (c) shorted patch antennas.

TABLE 7. Evaluation of the most suitable planar antenna designs for inter pico satellite communications.

	Shorted patch antenna	*Asymmetric E-shaped patch antenna*	*CPW-feed square slot antenna*
Volume	Small	Small	Small
Gain at 2.45 GHz	Low	High	Very low
BW	Wide	Wide	small
S_{11}	Small	Very small	Very high
Robustness	Weak	Weak	Strong
Beam steerability	Not steerable	Not steerable	Not steerable
Affordability (cost)	Cheap	Cheap	Cheap

steerability, and affordability. We see that all three designs are relatively small, have wide bandwidth, and are cheap. These antennas, however, are non-steerable and are not designed to operate at 2.45 GHz. We see that the asymmetric E-shaped patch antenna design has a superior gain over the shorted patch and CPW-feed square slot antennas. This is important as it enables long distance communications. Consequently, with the use of these antennas, fewer CubeSats will be required to participate in a swarm. Alternatively, they allow a swarm to operate over a large area. Another advantage of the asymmetric E-shaped patch antenna design is its very small return loss, meaning more power is radiated into space and less power is reflected.

Shorted patch, asymmetric E-shaped microstrip patch and CPW-feed square slot antennas can have different placement configurations on a 2U CubeSat. For satellite to ground station communication, placing an antenna on only one CubeSat face is sufficient. One example is to use an array on one face of the CubeSat for ground station communications [30]. This antenna should always be pointed to the ground station. This can be achieved by orienting the CubeSat using magnetic torqueing. Another configuration enables satellite-to-satellite (cross-link) communications. This will require more than one antenna on multiple faces of a CubeSat. As an example, the authors of [40] propose to place an individual antenna on each face of a 3U CubeSat.

V. CONCLUSION AND FUTURE WORK

We have presented the first comprehensive survey of small microstrip patch and slot antennas. These antennas are light,

small in size and achieve circular and cross polarization. Thus, they are most suited for use on pico-satellites. We have provided an extensive qualitative comparison of both antenna designs in terms of their features, design challenges, limitations, advantages and performance. We identify a number of open problems. First, most of the reviewed designs are non-steerable. Second, current microstrip patch antennas have higher gains and wider bandwidth than slot antennas. Third, the use of quarter wave depth cavities incurs additional weight, is expensive to construct and is difficult to integrate with planar circuits. Fourth, further research is required to achieve better impedance matching without the use of an external network, which adds weight and increases design complexity. In addition, this paper also contains an evaluation of the following antennas on a common platform: shorted patch, CPW-feed square slot and asymmetric E-shaped antenna. In particular, we evaluate the effect of a 2U CubeSat body on their performance. Our results show that the performance of the CPW-feed square slot antenna is affected significantly by the 2U CubeSat body if due care is not taken. We propose to use a PVC plastic sheet between the antenna and the CubeSat body to overcome this problem and to improve performance. Finally, we find that the asymmetric E-shaped patch antenna design to be the most suitable design for pico-satellite communications. It achieved a high gain of 7.3 dB, wide bandwidth of 2300 MHz and has a small size; i.e., 34×13 mm^2.

REFERENCES

[1] C. Underwood, V. Lappas, A. da Silva Curiel, M. Unwin, A. Baker, and M. Sweeting, "Science mission scenarios using 'palmsat' picosatellite technologies," in *Proc. 18th Annu. AIAA/USU Conf. Small Satellites*, Logan, UT, USA, 2004, pp. 1–11.

[2] R. Sandau, "Status and trends of small satellite missions for Earth observation," *Acta Astron.*, vol. 66, nos. 1–2, pp. 1–12, Jan./Feb. 2010.

[3] *National Aeronautics and Space Administration (NASA)*. [Online]. Available: http://www.nasa.gov/index.html, accessed Mar. 1, 2015.

[4] L. J. DeLucas, "International space station," *Acta Astron.*, vol. 38, nos. 4–8, pp. 613–619, Feb./Apr. 1996.

[5] R. Fdhila, T. M. Hamdani, and A. M. Alimi, "A multi objective particles swarm optimization algorithm for solving the routing pico-satellites problem," in *Proc. IEEE Int. Conf. Syst., Man, Cybern.*, Seoul, Korea, Oct. 2012, pp. 1402–1407.

[6] H. Heidt, J. Puig-Suari, A. S. Moore, S. Nakasuka, and R. Twiggs, "CubeSat: A new generation of picosatellite for education and industry low-cost space experimentation," in *Proc. 14th Annu. USU Conf. Small Satellites*, Logan, UT, USA, 2000, pp. 1–19.

[7] J. Puig-Suari, C. Turner, and R. Twiggs, "CubeSat: The development and launch support infrastructure for eighteen different satellite customers on one launch," in *Proc. 15th Annu. USU Conf. Small Satellites*, Logan, UT, USA, 2001, pp. 1–5.

[8] Surrey Satellite technology Ltd. *STRaND-1: Smartphone Nanosatellite*. [Online]. Available: http://www.sstl.co.uk, accessed Feb. 20, 2014.

[9] L. Reyneri, C. Sansoè, D. Del Corso, C. Passerone, S. Speretta, and M. Tranchero, "PicPot: A small satellite with educational goals," in *Proc. 18th EAEEIE Conf. Innov. Edu. Elect. Inf. Eng.*, Turin, Italy, Jul. 2007, pp. 1–4.

[10] R. Sandau and K. Brieß, "Potential for advancements in remote sensing using small satellites," in *Proc. Int. Arch., Photogramm., Remote Sens. Spatial Inf. Sci.*, Beijing, China, 2008, pp. 1–6.

[11] Surrey Space Centre. *Disaster Monitoring Constellation*. [Online]. Available: http://www.ee.surrey.ac.uk/SSC/, accessed Nov. 5, 2013.

[12] *An International Network of 50 CubeSats Project*. [Online]. Available: https://www.qb50.eu/, accessed Oct. 24, 2015.

[13] H. Bedon, C. Negron, J. Llantoy, C. M. Nieto, and C. O. Asma, "Preliminary internetworking simulation of the QB50 cubesat constellation," in *Proc. IEEE Conf. Commun.*, Bogotá, Colombia, Sep. 2010, pp. 1–6.

[14] J.-H. Huang, T.-Y. Lin, C.-M. Liu, and J.-C. Juang, "Design and evaluation of the attitude control system of the PHOENIX CubeSat," in *Proc. CACS Int. Automat. Control Conf.*, Nantou, Taiwan, Dec. 2013, pp. 47–51.

[15] A. Scholz, W. Ley, B. Dachwald, J. J. Miau, and J. C. Juang, "Flight results of the COMPASS-1 picosatellite mission," *Acta Astron.*, vol. 67, nos. 9–10, pp. 1289–1298, Nov./Dec. 2010.

[16] G. Mantzouris, "Micro and pico satellites in maritime security operations," *J. Naval Sci. Eng.*, vol. 8, no. 2, pp. 1–30, 2012.

[17] K. Woellert, P. Ehrenfreund, A. J. Ricco, and H. Hertzfeld, "Cubesats: Cost-effective science and technology platforms for emerging and developing nations," *Adv. Space Res.*, vol. 47, no. 4, pp. 663–684, Feb. 2011.

[18] J. A. King, J. Ness, G. Bonin, M. Brett, and D. Faber, "Nanosat Ka-band communications—A paradigm shift in small satellite data throughput," in *Proc. 26th Annu. AIAA Conf. Small Satellites*, Logan, UT, USA, Aug. 2012, pp. 1–21.

[19] S. Gao *et al.*, "Antennas for modern small satellites," *IEEE Antennas Propag. Mag.*, vol. 51, no. 4, pp. 40–56, Aug. 2009.

[20] X. Chen, C. G. Parini, B. Collins, Y. Yao, and M. U. Rehman, Eds., *Antennas for Global Navigation Satellite Systems*. Chichester, U.K.: Wiley, 2012.

[21] P. Muri, O. Challa, and J. McNair, "Enhancing small satellite communication through effective antenna system design," in *Proc. Military Commun. Conf.*, Oct./Nov. 2010, pp. 347–352.

[22] B. Murakami, A. Ohta, M. Tamamoto, G. Shiroma, R. Miyamoto, and W. Shiroma, "Self-steering antenna arrays for distributed picosatellite networks," in *Proc. 17th Annu. AIAA Conf. Small Satellites*, Logan, UT, USA, Aug. 2003, pp. 1–5.

[23] C. Y. Chiu, K. M. Shum, C.-H. Chan, and K. M. Luk, "Bandwidth enhancement technique for quarter-wave patch antennas," *IEEE Antennas Wireless Propag. Lett.*, vol. 2, no. 1, pp. 130–132, Feb. 2003.

[24] F. Ferrero, C. Luxey, R. Staraj, G. Jacquemod, M. Yedlin, and V. Fusco, "A novel quad-polarization agile patch antenna," *IEEE Trans. Antennas Propag.*, vol. 57, no. 5, pp. 1563–1567, May 2009.

[25] F. Rahmadani and A. Munir, "Microstrip patch antenna miniaturization using artificial magnetic conductor," in *Proc. IEEE 6th Int. Conf. Telecommun. Syst. Services Appl.*, Kuta, Bali, Indonesia, Oct. 2011, pp. 219–223.

[26] A. Holub and M. Polivka, "A novel microstrip patch antenna miniaturization technique: A meanderly folded shorted-patch antenna," in *Proc. 24th IEEE Conf. Microw. Techn.*, Prague, Czech Republic, Apr. 2008, pp. 1–4.

[27] W. Liao and Q.-X. Chu, "CPW-fed square slot antenna with lightening-shaped feedline for broadband circularly polarized radiation," *Prog. Electromagn. Res.*, vol. 18, pp. 61–69, Oct. 2010.

[28] H. Malekpoor and S. Jam, "Enhanced bandwidth of shorted patch antennas using folded-patch techniques," *IEEE Antennas Wireless Propag. Lett.*, vol. 12, pp. 198–201, Feb. 2013.

[29] N. Behdad and K. Sarabandi, "Bandwidth enhancement and further size reduction of a class of miniaturized slot antennas," *IEEE Trans. Antennas Propag.*, vol. 52, no. 8, pp. 1928–1935, Aug. 2004.

[30] A. Nascetti, E. Pittella, P. Teofilatto, and S. Pisa, "High-gain S-band patch antenna system for earth-observation CubeSat satellites," *IEEE Antennas Wireless Propag. Lett.*, vol. 14, pp. 434–437, Nov. 2015.

[31] R. Addaci, A. Diallo, P. L. Thuc, and R. Staraj, "Efficient miniaturization technique for wire patch antennas," *Microw. Opt. Technol. Lett.*, vol. 54, no. 5, pp. 1325–1327, May 2012.

[32] R. Azadegan and K. Sarabandi, "Design of miniaturized slot antennas," in *Proc. IEEE Antennas Propag. Soc. Int. Symp.*, vol. 4. Jul. 2001, pp. 565–568.

[33] R. Azadegan and K. Sarabandi, "Miniaturized folded-slot: An approach to increase the bandwidth and efficiency of miniaturized slot antennas," in *Proc. Antennas Propag. Soc. Int. Symp.*, vol. 4. 2002, pp. 14–17.

[34] R. O. Ouedraogo, E. J. Rothwell, A. R. Diaz, K. Fuchi, and A. Temme, "Miniaturization of patch antennas using a metamaterial-inspired technique," *IEEE Trans. Antennas Propag.*, vol. 60, no. 5, pp. 2175–2182, May 2012.

[35] S. A. Razavi and M. H. Neshati, "Development of a low-profile circularly polarized cavity-backed antenna using HMSIW technique," *IEEE Trans. Antennas Propag.*, vol. 61, no. 3, pp. 1041–1047, Mar. 2013.

[36] J.-S. Row, "The design of a squarer-ring slot antenna for circular polarization," *IEEE Trans. Antennas Propag.*, vol. 53, no. 6, pp. 1967–1972, Jun. 2005.

[37] D. Sievenpiper, H.-P. Hsu, and R. M. Riley, "Low-profile cavity-backed crossed-slot antenna with a single-probe feed designed for 2.34-GHz satellite radio applications," *IEEE Trans. Antennas Propag.*, vol. 52, no. 3, pp. 873–879, Mar. 2004.

[38] W. Hong, N. Behdad, and K. Sarabandi, "Size reduction of cavity-backed slot antennas," *IEEE Trans. Antennas Propag.*, vol. 54, no. 5, pp. 1461–1466, May 2006.

[39] H. Malekpoor and S. Jam, "Miniaturised asymmetric E-shaped microstrip patch antenna with folded-patch feed," *IET Microw. Antennas Propag.*, vol. 7, no. 2, pp. 85–91, Jan. 2013.

[40] A. Budianu, T. J. W. Castro, A. Meijerink, and M. J. Bentum, "Inter-satellite links for cubesats," in *Proc. IEEE Conf. Aerosp.*, Big Sky, MT, USA, Mar. 2013, pp. 1–10.

[41] G. Di Massa and G. Mazzarella, "Shorted annular patch antenna," *Microw. Opt. Technol. Lett.*, vol. 8, no. 4, pp. 222–226, Mar. 1995.

[42] H. Iwasaki, "A circularly polarized small-size microstrip antenna with a cross slot," *IEEE Trans. Antennas Propag.*, vol. 44, no. 10, pp. 1399–1401, Oct. 1996.

[43] K.-L. Wong, C.-C. Huang, and W.-S. Chen, "Printed ring slot antenna for circular polarization," *IEEE Trans. Antennas Propag.*, vol. 50, no. 1, pp. 75–77, Jan. 2002.

[44] S.-L. Ma, C. J. Shih, and J.-S. Row, "Four-element microstrip array with polarization diversity," *Microw. Opt. Technol. Lett.*, vol. 55, no. 7, pp. 1653–1657, Jul. 2013.

[45] T. J. Mizuno *et al.*, "Antennas for distributed nanosatellite networks," in *Proc. IEEE/ACES. Int. Conf. Wireless Commun. Appl. Comput. Electromagn.*, Hawaii, HI, USA, Apr. 2005, pp. 606–609.

[46] R. Azadegan and K. Sarabandi, "Bandwidth enhancement of miniaturized slot antennas using folded, complementary, and self-complementary realizations," *IEEE Trans. Antennas Propag.*, vol. 55, no. 9, pp. 2435–2444, Sep. 2007.

[47] R. M. Rodriguez-Osorio and E. F. Ramírez, "A hands-on education project: Antenna design for inter-CubeSat communications [education column]," *IEEE Antennas Propag. Mag.*, vol. 54, no. 5, pp. 211–224, Oct. 2012.

[48] J.-S. Row and C.-J. Shih, "Polarization-diversity ring slot antenna with frequency agility," *IEEE Trans. Antennas Propag.*, vol. 60, no. 8, pp. 3953–3957, Aug. 2012.

[49] Y.-J. Hu, W.-P. Ding, and W.-Q. Cao, "Broadband circularly polarized microstrip antenna array using sequentially rotated technique," *IEEE Antennas Wireless Propag. Lett.*, vol. 10, pp. 1358–1361, Nov. 2011.

[50] Y. Qian, D. Sievenpiper, V. Radisic, E. Yablonovitch, and T. Itoh, "A novel approach for gain and bandwidth enhancement of patch antennas," in *Proc. IEEE Conf. Radio Wireless*, Colorado Springs, CO, USA, Aug. 1998, pp. 221–224.

[51] R. Montaño *et al.*, "Development of low-profile antennas for CubeSats," in *Proc. 28th Annu. AIAA/USU Conf. Small Satellite*, Logan, UT, USA, Aug. 2014, pp. 1–5.

[52] B. Ghosh, S. K. M. Haque, and N. R. Yenduri, "Miniaturization of slot antennas using wire loading," *IEEE Antennas Wireless Propag. Lett.*, vol. 12, no. 5, pp. 488–491, Apr. 2013.

[53] T.-Y. Lee and J.-S. Row, "Frequency reconfigurable circularly polarized slot antennas with wide tuning range," *Microw. Opt. Technol. Lett.*, vol. 53, no. 7, pp. 1501–1505, Jul. 2011.

[54] Z.-H. Tu, Q.-X. Chu, and Q.-Y. Zhang, "High-gain slot antenna with parasitic patch and windowed metallic superstrate," *Prog. Electromagn. Res. Lett.*, vol. 15, pp. 27–36, 2010.

[55] I. Singh and D. V. Tripathi, "Micro strip patch antenna and its applications: A survey," *Int. J. Comput. Technol. Appl.*, vol. 2, no. 5, pp. 1595–1599, 2011.

[56] S. Shrestha, M. Agarwal, P. Ghane, and K. Varahramyan, "Flexible microstrip antenna for skin contact application," *Int. J. Antennas Propag.*, Jun. 2012, Art. ID 745426.

[57] C. Y. Chiu, C. H. Chan, and K. M. Luk, "Study of a small wide-band patch antenna with double shorting walls," *IEEE Antennas Wireless Propag. Lett.*, vol. 3, no. 1, pp. 230–231, Dec. 2004.

[58] C. Y. Chiu, H. Wong, and C. H. Chan, "Study of small wideband folded-patch-feed antennas," *IET Microw. Antennas Propag.*, vol. 1, no. 2, pp. 501–505, Apr. 2007.

[59] S. Gao, A. Sambell, and S. S. Zhong, "Polarization-agile antennas," *IEEE Antennas Propag. Mag.*, vol. 48, no. 3, pp. 28–37, Jun. 2006.

[60] F. Jolani, A. M. Dadgarpour, and H. R. Hassani, "Compact M-slot folded patch antenna for WLAN," *Prog. Electromagn. Res. Lett.*, vol. 3, pp. 35–42, 2008.

[61] W. Richards, Y. Lo, and D. Harrison, "An improved theory for microstrip antennas and applications," *IEEE Trans. Antennas Propag.*, vol. 29, no. 1, pp. 38–46, Jan. 1981.

[62] P. Salonen, M. Keskilammi, and M. Kivikoski, "New slot configurations for dual-band planar inverted-F antenna," *Microw. Opt. Technol. Lett.*, vol. 28, no. 5, pp. 293–298, Mar. 2001.

[63] J. Lange, "Interdigitated stripline quadrature hybrid (correspondence)," *IEEE Trans. Microw. Theory Techn.*, vol. 17, no. 12, pp. 1150–1151, Dec. 1969.

[64] H. Oraizi and A.-R. Sharifi, "Design and optimization of broadband asymmetrical multisection wilkinson power divider," *IEEE Trans. Microw. Theory Techn.*, vol. 54, no. 5, pp. 2220–2231, May 2006.

[65] E. J. Wilkinson, "An N-way hybrid power divider," *IRE Trans. Microw. Theory Techn.*, vol. 8, no. 1, pp. 116–118, Jan. 1960.

[66] D. S. Goshi, K. M. K. H. Leong, and T. Itoh, "Recent advances in retrodirective system technology," in *Proc. IEEE Conf. Radio Wireless Symp.*, San Diego, CA, USA, Oct. 2006, pp. 459–462.

[67] K. M. K. H. Leong, R. Y. Miyamoto, and T. Itoh, "Moving forward in retrodirective antenna arrays," *IEEE Potentials*, vol. 22, no. 3, pp. 16–21, Aug./Sep. 2003.

[68] R. Y. Miyamoto and T. Itoh, "Retrodirective arrays for wireless communications," *IEEE Microw. Mag.*, vol. 3, no. 1, pp. 71–79, Mar. 2002.

[69] R. Coccioli, F.-R. Yang, K.-P. Ma, and T. Itoh, "Aperture-coupled patch antenna on UC-PBG substrate," *IEEE Trans. Microw. Theory Techn.*, vol. 47, no. 11, pp. 2123–2130, Nov. 1999.

[70] R. Gonzalo, P. de Maagt, and M. Sorolla, "Enhanced patch-antenna performance by suppressing surface waves using photonic-bandgap substrates," *IEEE Trans. Microw. Theory Techn.*, vol. 47, no. 11, pp. 2131–2138, Nov. 1999.

[71] M. Rahman and M. A. Stuchly, "Circularly polarised patch antenna with periodic structure," *IEE Proc. Microw., Antennas Propag.*, vol. 149, no. 3, pp. 141–146, Jun. 2002.

[72] M. J. Vaughan, K. Y. Hur, and R. C. Compton, "Improving radiation pattern of microstrip antennas," *IEEE Trans. Antennas Propag.*, vol. 42, no. 6, pp. 882–885, Jun. 1994.

[73] H.-Y. D. Yang and J. Wang, "Surface waves of printed antennas on planar artificial periodic dielectric structures," *IEEE Trans. Antennas Propag.*, vol. 49, no. 3, pp. 444–450, Mar. 2001.

[74] E. Yablonovitch, "Photonic band-gap structures," *J. Opt. Soc. Amer. B.*, vol. 10, no. 2, pp. 283–295, 1993.

[75] K.-F. Tong and J. Huang, "New proximity coupled feeding method for reconfigurable circularly polarized microstrip ring antennas," *IEEE Trans. Antennas Propag.*, vol. 56, no. 7, pp. 1860–1866, Jul. 2008.

[76] A. Tiburcio-Silver, A. Sanchez-Juarez, and A. Avila-Garcia, "Properties of gallium-doped ZnO deposited onto glass by spray pyrolysis," *Solar Energy Mater. Solar Cells*, vol. 55, nos. 1–2, pp. 3–10, Jul. 1998.

[77] K. Schilling, "Earth observation by distributed networks of small satellites," in *Proc. IEEE Int. Conf. Instrum. Commun. Inf. Technol. Biomed. Eng. (ICICI-BME)*, Bandung, Indonesia, Nov. 2009, pp. 1–3.

[78] A. Alù, F. Bilotti, N. Engheta, and L. Vegni, "Subwavelength, compact, resonant patch antennas loaded with metamaterials," *IEEE Trans. Antennas Propag.*, vol. 55, no. 1, pp. 13–25, Jan. 2007.

[79] F. Bilotti, A. Alu, and L. Vegni, "Design of miniaturized metamaterial patch antennas with μ-negative loading," *IEEE Trans. Antennas Propag.*, vol. 56, no. 6, pp. 1640–1647, Jun. 2008.

[80] A. Erentok, P. L. Luljak, and R. W. Ziolkowski, "Characterization of a volumetric metamaterial realization of an artificial magnetic conductor for antenna applications," *IEEE Trans. Antennas Propag.*, vol. 53, no. 1, pp. 160–172, Jan. 2005.

[81] H. Mosallaei and K. Sarabandi, "Design and modeling of patch antenna printed on magneto-dielectric embedded-circuit metasubstrate," *IEEE Trans. Antennas Propag.*, vol. 55, no. 1, pp. 45–52, Jan. 2007.

[82] G. A. Conway and W. G. Scanlon, "Antennas for over-body-surface communication at 2.45 GHz," *IEEE Trans. Antennas Propag.*, vol. 57, no. 4, pp. 844–855, Apr. 2009.

[83] J. Wang, "Zigbee light link and its applications," *IEEE Wireless Commun.*, vol. 20, no. 4, pp. 6–7, Aug. 2013.

[84] A. P. Feresidis, G. Goussetis, S. Wang, and J. C. Vardaxoglou, "Artificial magnetic conductor surfaces and their application to low-profile high-gain planar antennas," *IEEE Trans. Antennas Propag.*, vol. 53, no. 1, pp. 209–215, Jan. 2005.

[85] L. K. Fong and R. Chair, "On the use of shorting pins in the design of microstrip patch antennas," *Hong Kong Inst. Eng. (HKIE) Trans.*, vol. 11, no. 4, pp. 31–38, Jun. 2004.

[86] L. C. Kempel, "Radiation by cavity-backed antennas on a circular cylinder," *IEE Proc. Microw., Antennas Propag.*, vol. 142, no. 3, pp. 233–239, Jun. 1995.
[87] B. Liu, W. Hong, Y.-Q. Wang, Q.-H. Lai, and K. Wu, "Half mode substrate integrated waveguide (HMSIW) 3-dB coupler," *IEEE Microw. Wireless Compon. Lett.*, vol. 17, no. 1, pp. 22–24, Jan. 2007.
[88] F. Ferrero, C. Luxey, R. Staraj, G. Jacquemod, M. Yedlin, and V. Fusco, "Theory and design of a tunable quasi-lumped quadrature coupler," *Microw. Opt. Technol. Lett.*, vol. 51, no. 9, pp. 2219–2222, Sep. 2009.
[89] A. U. Bhobe, C. L. Holloway, M. Piket-May, and R. Hall, "Wide-band slot antennas with CPW feed lines: Hybrid and log-periodic designs," *IEEE Trans. Antennas Propag.*, vol. 52, no. 10, pp. 2545–2554, Oct. 2004.
[90] J.-S. Chen, "Dual-frequency annular-ring slot antennas fed by CPW feed and microstrip line feed," *IEEE Trans. Antennas Propag.*, vol. 53, no. 1, pp. 569–573, Jan. 2005.
[91] X.-C. Lin and C.-C. Yu, "A dual-band CPW-fed inductive slot-monopole hybrid antenna," *IEEE Trans. Antennas Propag.*, vol. 56, no. 1, pp. 282–285, Jan. 2008.
[92] Z. C. Ioannidis, O. Dumbrajs, and I. G. Tigelis, "Eigenvalues and ohmic losses in coaxial gyrotron cavity," *IEEE Trans. Plasma Sci.*, vol. 34, no. 4, pp. 1516–1522, Aug. 2006.
[93] *High Frequency Structure Simulator (HFSS)*. [Online]. Available: http://www.ansys.com/, accessed Jun. 30, 2015.
[94] K. Arunachalam, P. Maccarini, T. Juang, C. Gaeta, and P. R. Stauffer, "Performance evaluation of a conformal thermal monitoring sheet sensor array for measurement of surface temperature distributions during superficial hyperthermia treatments," *Int. J. Hyperthermia*, vol. 24, no. 4, pp. 313–325, Dec. 2008.

FAISEL EM TUBBAL (M'14) was born in Libya in 1978. He received the B.S. degree in electronics engineering from the Tripoli College of Electronic Technology, Ben Ashour, Tripoli, Libya, the Advanced Graduate Diploma and M.S. degrees in Telecommunication Engineering from the University of Wollongong, Australia, in 2011 and 2012, respectively, and the M.S. degree in engineering management from the University of Wollongong, in 2013, where he is currently pursuing the Ph.D. degree in telecommunication engineering. He has been a Researcher with the Libyan Centre for Remote Sensing and Space Science, Tripoli, Libya. He is also an Academic Assistant with the School of Electrical, Computer and Telecommunication Engineering, University of Wollongong. He is interested in planar antenna designs and CubeSat communications.

RAAD RAAD received the B.E. (Hons.) degree from the University of Wollongong, Australia, in 1997. His Ph.D. thesis was entitled Neuro-Fuzzy Logic Admission Control in Cellular Mobile Networks in 2006. He has over five years of industrial research experience and another five years of experience in academic research. He has authored five U.S. patent filings of which three have been granted and over 50 refereed publications and technical reports. His expertise is in wireless communications with a focus on medium access control (MAC) and bandwidth management protocols for wireless networks. He has led and collaborated on significant projects in the areas of sensor networks, the IEEE 802.11, the IEEE 802.15.3, MeshLAN, RFIDs, and cellular networks. The technical areas that he covered during the numerous projects include admission control, bandwidth management, low-power MAC protocols, and routing protocols.

KWAN-WU CHIN received the B.Sc. and Ph.D. (Hons.) degrees from the Curtin University of Technology, Australia. He was the vice chancellor's commendation. After obtaining the Ph.D., degree he joined the Motorola Research Laboratory as a Senior Research Engineer, where he developed zero-configuration home networking protocols and designed new medium access control protocols for wireless sensors networks. In 2004, he joined the University of Wollongong as a Senior Lecturer. He was subsequently promoted to Associate Professor in 2011. He holds four patents, and has authored over 100 articles in numerous conferences and journals. His current areas include medium access control protocols for wireless networks, routing protocols for delay tolerant networks, RFID anti-collision protocols, and resources management issues in wireless networks.